SIN-CHN
SCIENTIFIC PRESS PTE.LTD.

Molecular & Cellular Biomechanics 2024, 21, 138.
https://doi.org/10.62617/mcb.v21.138

Article

HSP90AB1's effect on hepatocellular carcinoma's local immune response and prognosis

Yudong Wang

Research Institute, Beijing Wandong Medical Technology Co., Ltd., Beijing 110000, China; wangyudong927@163.com

CITATION

Wang Y. HSP90AB1's effect on hepatocellular carcinoma's local immune response and prognosis. Molecular & Cellular Biomechanics. 2024; 21: 138. https://doi.org/10.62617/mcb.v21.138

ARTICLE INFO

Received: 9 May 2024
Accepted: 18 June 2024
Available online: 13 August 2024

Abstract: Background: HSP90AB1 (heat shock protein 90 kDa alpha, class B, member 1) helps collapsing proteins, and the restraint of HSP90AB1 is anticipated to successfully illuminate the issue of warm stun reaction of the restraint of HSP90. The fundamental component by which HSP90AB1 influences the neighbourhood-resistant reaction to tumours remains vague. **Materials and strategies:** This investigation analyzes the impact of HSP90AB1 on the composition and dispersion of safe cell invades inside hepatocellular carcinoma (HCC) tissues. At that point, by examining HSP90AB1-associated immunoregulatory qualities, KDR, MICB, and TNFRSF4 were distinguished as critical supporters. A prognostic show joining these qualities was built, and its exactness was approved by utilizing free datasets from the ICGC and TCGA databases. **Results:** Our discoveries illustrate that the restraint of HSP90AB1 expanded the penetration of CD8+ T cells and other resistant cell populaces inside HCC tissues. This improved resistant reaction was related to moving forward with a quiet prognosis, proposing a potential restorative procedure for HCC. **Conclusion:** We propose that focusing on HSP90AB1 may improve the survival results of HCC patients by encouraging safe cell penetration into the tumour microenvironment.

Keywords: HCC; HSP90AB1; immunotherapy; PD-1; CD8; prognosis

1. Introduction

Hepatocellular carcinoma (HCC), the seventh most common cancer universally, is the moment-driving cause of passing from cancer, highlighting its critical effect on open well-being [1,2]. HCC's worldwide prognosis remains distressing, with dreariness and mortality rates floating close to equality. In 2018, gauges put the worldwide horribleness of liver cancer at 9.3 per thousand, closely reflecting its mortality rate of 8.5 per thousand, highlighting the critical burden of this malady [1]. The expanding world predominance of NAFLD/NASH could be a major open well-being issue, and it is anticipated to end up being the essential cause of HCC, which is all-inclusive, outperforming viral components. This underscores the significance of creating viable avoidance and treatment approaches for NAFLD/NASH-related HCC [3]. As immunotherapy develops as a potential treatment for HCC, analysts are progressively centring on optimizing its combination with neighbourhood treatments. This centre on combination techniques reflects the potential of synergistic impacts in making strides in understanding results [4]. Immunotherapy can potentially treat different cancers, but its adequacy is still restricted to a few patients. This confinement has fueled a surge of inquiries about investigating effective, helpful approaches to improve the adequacy of immunotherapy. These endeavours, which are focused on overcoming the restrictions of immunotherapy alone, have become a major centre of current investigative endeavours [5]. Among the different components of the activity

of HSP90 inhibitors, their capacity to upgrade immunotherapy results has gotten impressive consideration. The capacity of HSP90 inhibitors to change the tumour microenvironment and possibly move forward the viability of immunotherapies has gathered noteworthy consideration [6].

HSP90AB1, an atomic chaperone, is crucial in keeping up the auxiliary keenness and usefulness of various cellular proteins, especially receptors, by encouraging their appropriate collapsing and empowering viable signaling. Whereas HSPs, counting HSP90AB1, maintain protein homeostasis and back cellular capacities, they can also incomprehensibly contribute to tumorigenesis and cell multiplication. Within the nonappearance of HSPs, changed receptor proteins ended up unsteady and debase, driving uncontrolled signaling pathways and tumour development, highlighting the complex part of HSPs in typical cellular work and malady forms [7]. Focusing on HSP90AB1 has appeared helpful for different conditions, such as malignancies, provocative maladies, and hereditary disarrangements [8]. By focusing on the HSP90 protein collapsing component, inhibitors can simultaneously viably disturb different carcinogenic signaling pathways, advertising a combinatorial approach to cancer treatment [9]. Novel HSP90 inhibitors focusing on the C-terminal space have appeared to guarantee overcoming impediments related to N-terminal inhibitors [10], which have, as of now, illustrated helpful potential in clinical trials [11].

Later inquiries about utilizing mouse tumour models have uncovered that HSP90 hindrance not as it specifically impacts tumour cell survival but, moreover, in a roundabout way, improves anti-tumour resistance by balancing the tumour microenvironment, particularly by diminishing PD-L1 expression on tumour cells and expanding the nearness of actuated CD8+ T cells inside the tumour. The continuous investigation of the complicated relationship between HSP90AB1 and the tumor-safe microenvironment fills the improvement of progressed HSP90 inhibitors with upgraded specificity and viability, holding monstrous potential for revolutionizing cancer treatment [12]. Thinks have illustrated that HSP90 inhibitors, such as Ganetespib, can increase the cytotoxic impacts of autologous T-cells against melanoma cells and make strides in reactions to safe checkpoint inhibitors, demonstrating their potential as a complementary methodology to boost the execution of current immunotherapies [13]. Preclinical studies have illustrated the potential of other HSP90 inhibitors, such as17-DMAG (17-dimethylaminoethylamino-17-normethoxygeldanamycin), in abating tumour development, upgrading tumour cell acknowledgement by antigen-specific CD8+ T cells, and balancing the resistant cell composition inside the tumour microenvironment [14,15]. In vitro, 17-DMAG treatment moved forward the acknowledgement of tumour cells by EphA2-specific CD8+ T cells, whereas in vivo administration altered the adjustment of resistant cell populaces, favouring CD8+ T cells over immunosuppressive cell sorts, assisting emphasizing the immunomodulatory effect of HSP90 restraint [16].

HSP90 restraint has the potential to advantageously tweak the tumour-resistant microenvironment by modifying the adjustment of resistant cell populaces, subsequently cultivating a more compelling anti-tumour-resistant reaction. Furthermore, HSP90 restraint can lead to the proteasomal debasement of HER2, coming about within the introduction of MHC-enhanced antigenic peptides recognized and focused on by CD8+ T cells, contributing to the anti-tumour safe

reaction. This component emphasizes the potential of HSP90 hindrance to extend tumour cell permeability to the safe framework, hence upgrading the viability of T cell-mediated anti-tumour reactions. The nearness of T and NK lymphocytes was essentially expanded inside the tumour microenvironment of syngeneic C3H mice. Ponders have illustrated that within the nonappearance of immunotherapy, the organization of a tall measurement (10 μg) of geldanamycin brought about noteworthy tumour development restraint in syngeneic C3H mice, though a moo measurement (2.5 μg) of geldanamycin driven to a lessening in HER2 expression without affecting tumour estimate. Our ponder appears that combining a DNA immunization focusing on p185neu with a moo dosage of geldanamycin (GA) altogether makes strides in the general survival of syngeneic C3H mice.

The moved forward survival is ascribed to an expanded nearness of CD8+ T-lytic cells and a lessening of CD4+ T cells, possibly diminishing Treg cell numbers and improving CD8+ murdering movement. Our inquiry recommends that halfway restraint of pleiotropic impacts may permit low-dose medicines to improve tumour-specific resistant reactions through different instruments, such as moved forward tumour antigen preparing and introduction, expanded MHC show thickness, and raised atomic figure kappa light chain enhancer of enacted B cells (NFκB) signaling. These instruments collectively contribute to stifling the tumour microenvironment and expanding common executioner (NK) cell focusing [17]. An audit of past considerations on the impacts of HSP90 inhibitors on tumour resistance reliably shows improved resistant reactions after treatment with moo inhibitor dosages. This perception proposes that low-dose regimens, possibly in conjunction with the special aggregation of these drugs inside the tumour microenvironment, may be adequate to initiate atomic changes inside the tumour that upgrade anti-tumour resistance without compromising systemic safe work [18]. HSP90 restraint has illustrated the capacity to stifle CD4+ T cell expansion in both murine and human in vitro blended lymphocyte responses. Geldanamycin (GA), a normal HSP90 inhibitor, improves MHC course I antigen introduction through the ubiquitin-proteasome pathway, coming about in expanded invasion of CD8+ T cells and normal executioner (NK) cells into tumours, rendering them more vulnerable to cytotoxic impacts [19]. This proposed component highlights the potential of GA to encourage immune-mediated acknowledgement and disposal of tumour cells, contributing to its anti-tumour action. Be that as it may, GA also shows poisonous qualities towards refined T cells by downregulating protein tyrosine kinase action, which is significant for T cell work. This double impact highlights the need for cautious optimization of GA-based treatments to maximize their anti-tumour potential while minimizing any hindering effect on T cell work. To tackle the immunomodulatory potential of GA while mitigating its toxic impacts on T cells, analysts may investigate techniques such as focused on conveyance frameworks, measurement optimization, or the advancement of GA subordinates with progressed selectivity. Optimizing the helpful methodology may empower an adjustment between boosting anti-tumour resistance and keeping up cytotoxic T cell work, possibly progressing cancer immunotherapy results [17].

Considers show that HSP90 restraint has the potential to overcome immunoresistance in tumours by enhancing their defenselessness to T-cell-mediated cytotoxicity, possibly through the concealment of PD-1 expression and the

reinvigoration of tumor-responsive T cells [20]. Hsp90 inhibitors display tumour-selective properties, permitting discontinuous dosing that keeps up effective chaperone hindrance inside the tumour and minimizing systemic presentation and potential immune-related antagonistic impacts [6]. The HSP90 inhibitor 17-AAG has appeared to fortify melanoma antigen expression, progressing T-cell acknowledgement and focusing on melanoma patients [21]. Combining 17-DMAG with agonistic EphA2 antibodies has synergistically moved tumour cell acknowledgement by CD8+ T cells, emphasizing the potential of HSP90 inhibitors in upgrading anti-tumour resistance [14]. Be that as it may, the effect of HSP90 inhibitors on the safe microenvironment in liver cancer remains generally unexplored. To bridge this hole, we comprehensively examined the affiliation between HSP90AB1 expression and the neighbourhood-resistant reaction in liver cancer utilizing clinical information from the TCGA database. Our examination uncovered resistant cell subpopulations that are strongly associated with HSP90AB1 expression levels. We recognized fundamental safe administrative qualities related to HSP90AB1 and created a prognostic demonstration based on these discoveries. The model's vigour was affirmed utilizing a free dataset from the ICGC database, highlighting the considerable effect of HSP90AB1 on the liver cancer-safe microenvironment and its potential as a prognostic biomarker and helpful target.

CDK1-SRC interaction-dependent transcriptional activation of HSP90AB1 promotes anti-tumor immunity in hepatocellular carcinoma [22]. Researchers used statistical methods, meta-analyses, and investigations of protein-protein interactions to determine which immunological genes were important and how they were related. Experimental evidence from both in vitro and in vivo settings supports the role of the CDK1-SRC-HSP90AB1 network in antitumor immunity and HCC development. Clinicopathological characteristics and immunological infiltration were used to create a predictive risk model. CCL20, ROBO1, BIRC5, and HSP90AB1 immune genes were important predictive markers. The CDK1-SRC connection stimulated HSP90AB1, which boosted HCC cell migration and proliferation via the CDK1-SRC-HSP90AB1 network. Reversing the impact of CDK1 and SRC on HCC was achieved by manipulating either SRC or HSP90AB1. Antitumor immunity and HCC tumour genesis were both affected by the CDK1-SRC-HSP90AB1 network. This research shows that the CDK1-SRC-HSP90AB1 network is an important immune-regulatory network in HCC prognosis.

A novel prognostic index of hepatocellular carcinoma based on immunogenomic landscape analysis [23]. The prognostic index's reliability was confirmed using data from the ICGC database. The results show that 54 IRGs with varied expression were strongly correlated with HCC prognosis and that their expression levels were inversely proportional to the difference in copy numbers. Functional enrichment analysis shows these genes are involved in signaling pathways relevant to tumours and the immune system. Five possible biomarkers were also found: IRG, MAPK3, HSP90AA1, HSP90AB1, HSPA4, and CDK4. Lastly, an innovative prognostic index was developed using IRGs (PSMD14, FABP6, ISG20L2, HGF, BIRC5, IL17D, and STC2), which functions as both a prognostic factor and an indicator of immune cell infiltration levels. By studying the genomes of IRGs in HCC and screening several clinically relevant IRGs, our team developed a model that effectively uses IRG-based

immunolabeling methods to classify and characterize patients, allowing for monitoring HCC prognoses.

2. Materials and strategies

2.1. Details the data sources (TCGA, ICGC)

Hepatocellular carcinoma (HCC) transcriptome information was procured from the TCGA database and isolated into HCC and typical bunches. At that point, quality identifiers were changed to compare quality names [24]. Clinical information was obtained and subjected to thorough investigation from the TCGA database. The comparative investigation of HSP90AB1 quality expression profiles in typical and HCC persistent cohorts uncovered stamped incongruities with measurable noteworthiness (**Figure 1**). To explain the potential suggestions of HSP90AB1 within the tumour-safe microenvironment, a comprehensive appraisal of resistant cell penetration designs was conducted by leveraging the rich transcriptomic information accessible within "The Cancer Genome Map" book (TCGA) database. This investigation yielded quantitative information on the plenitude of different resistant cell populations inside the tumour microenvironment. The discoveries were displayed in a bar chart for upgraded visualization (**Figure 2**). Each resistant cell populace was doled out a particular colour inside the bar chart, encouraging visually recognizable proof (**Figure 3**). To explain the complicated connections among these cell sorts, we built a comprehensive relationship chart, which revealed noteworthy affiliations between different safe cell populations. Moreover, patients were fastidiously separated into typical and HCC cohorts (**Figure 4**), empowering us to differentiate safe cell invasion designs between these particular bunches. The utilization of violin plots in **Figure 5** offers an outwardly instinctive representation of the perplexing varieties in safe cell penetration profiles watched between the ordinary and HCC cohorts. These graphical shows richly capture the dispersion and heterogeneity of safe cell subpopulations inside each gather, encouraging a nuanced appreciation of the differential resistant scene that characterizes these particular organic states and giving important experiences into the potential immunological underpinnings of HCC pathogenesis and movement. The TIMER database was utilized to comprehensively investigate the relationship between varieties in HSP90AB1 quality duplicate numbers and the invasion of different resistant cell populaces inside the tumour microenvironment [25]. To explain the useful results of HSP90AB1 quality expression modifications, we conducted a quality set improvement investigation (GSEA) utilizing the GSEA computer program. This comprehensive examination distinguished pathways altogether enhanced in affiliation with the up-and down-regulation of the HSP90AB1 quality, giving profitable bits of knowledge into the natural forms and atomic instruments possibly influenced by HSP90AB1 expression changes [26]. To examine the relationship between HSP90AB1 quality expression and lymphocyte invasion designs, a comprehensive relationship investigation was conducted utilizing the TISIDB database.

2.2. Analytical methods

The investigation yielded a relationship heatmap, which visualized the affiliations between HSP90AB1 expression levels and the wealth of different lymphocyte populaces over distinctive tumour sorts. This heatmap gives a worldwide outline of the potential effect of HSP90AB1 expression on the resistant cell composition inside the tumour microenvironment. To pick up a more point-by-point understanding of the relationship between HSP90AB1 expression and particular lymphocyte subtypes within the hepatocellular carcinoma (HCC) setting, a relationship diffuse plot was created utilizing information from HCC tissue tests. This centred examination permitted a more granular examination of how HSP90AB1 expression levels may impact the penetration of person lymphocyte subpopulations inside the HCC tumour microenvironment. Relationship coefficients were fastidiously calculated to measure the connections between HSP90AB1 quality, lymphocyte invasion, and immunoregulatory quality expression. These coefficients give a numerical degree of the quality and heading of the affiliations, empowering a more exact appraisal of the potential administrative part of HSP90AB1 in forming the resistant scene of tumours. Moreover, a comprehensive heatmap utilizing the TISIDB database was created to amplify the examination of past lymphocyte invasion. This heatmap visualized the relationships between HSP90AB1 expression levels and the expression designs of immunoregulatory qualities over an assorted run of tumour sorts. By joining this extra data layer, the heatmap gives profitable bits of knowledge into the potential transaction between HSP90AB1 and key immunoregulatory pathways in different cancer settings. Combining these examinations, counting the relationship heatmaps, scramble plots, and calculated relationship coefficients gave a strong and multifaceted approach to understanding the relationship between HSP90AB1 quality expression and the resistant microenvironment of tumours. These discoveries lay the establishment for advanced examinations into the potential part of HSP90AB1 as a modulator of safe cell penetration and immunoregulatory quality expression, with suggestions for the advancement of focused on immunotherapies and prognostic biomarkers in cancer [27]. A diffuse plot was fastidiously created to examine the complicated connections between HSP90AB1 quality expression and immunoregulatory pathways inside the HCC microenvironment. This visualization successfully captured the relationships between HSP90AB1 expression and the expression designs of differing immunoregulatory qualities. Besides, a comprehensive examination recognized immunoregulatory qualities showing co-expression with HSP90AB1, possibly uncovering critical affiliations that will contribute to our understanding of the complex exchange between HSP90AB1 and the tumor-safe scene in HCC. To pick up encouraging bits of knowledge into the complex protein interaction connections among immunoregulatory qualities co-expressed with HSP90AB1, we utilized the strong asset of STRING, a comprehensive database of protein-protein intuitive. This examination empowered the development of a nitty-gritty protein interaction organization, successfully visualizing the perplexing associations between these qualities. This arranged profitable experiences into the potential utilitarian connections and pathways related to the co-expressed immunoregulatory qualities, possibly uncovering novel knowledge into the

administrative components of the transaction between HSP90AB1 and the tumor-safe scene [28].

2.3. Evaluation methods

To explain the organic centrality and atomic components supporting the immunoregulatory qualities of intrigued, a multifaceted bioinformatic approach was utilized, leveraging the effective Web-based Quality Set Investigation Toolkit (WebGestalt). This comprehensive investigation enveloped a fastidious examination of quality philosophy (GO) comments, unravelling the overrepresented useful categories and cellular forms whereas concurrently conducting a careful pathway improvement investigation to distinguish the key signaling cascades and metabolic systems in which these qualities are embroiled. The integration of these complementary explanatory strategies given an all-encompassing see of the utilitarian scene and organic setting inside which these immunoregulatory qualities work, shedding light on their potential parts in forming the safe reaction and their broader suggestions for well-being and infection. The utilization of this modern approach empowered a comprehensive investigation of the quality set's useful scene, disclosing the overrepresented organic pathways, atomic components, and cellular compartments that collectively contribute to the watched phenotype, giving an all-encompassing see of the basic atomic system and its potential suggestions within the considered organic setting. The discoveries of this comprehensive examination shed light on the complicated relationship between HSP90AB1 and the resistant microenvironment inside the tumor, uncovering novel points of view on the potential components by which HSP90AB1 impacts resistant cell penetration and work, eventually contributing to a more profound understanding of the complex flow overseeing tumor movement and reaction to immunotherapeutic intercessions. By distinguishing the overrepresented GO terms and pathways, we revealed potential instruments through which HSP90AB1 and its related qualities contribute to the complicated intelligent between the tumor and the resistant framework. These discoveries shed light on the basic parts played by these qualities in forming the immunological milieu inside the tumor microenvironment, clearing the way for advance examinations and potential restorative intercessions in cancer immunology. Also, the distinguishing proof of altogether enhanced pathways shed light on the potential components fundamental to the co-expression designs watched, possibly uncovering novel restorative targets or prognostic biomarkers [29]. To explore the clinical pertinence of the recognized immunoregulatory qualities in depth, we performed a comprehensive prognostic investigation by joining their expression information with the survival information of clinical patients. This thorough examination uncovered a subset of qualities related to quiet prognosis, as delineated in a nitty gritty timberland outline. These prognostic qualities were utilized to build a solid prognostic demonstration, giving important experiences into the potential of these qualities as prognostic biomarkers or restorative targets. Utilizing the expression data of the qualities included in the prognostic show, an individualized chance score was computed for each quiet inside the TCGA cohort. This hazard score was the premise for dichotomizing patients into tall- and low-risk subgroups, with the middle hazard score acting as the stratification limit. Patients were

stratified into two unmistakable bunches based on their hazard scores: those with scores outperforming the middle edge were classified as high-risk, whereas those falling underneath the middle were doled out to the low-risk category.

2.4. Patient cohort

To completely assess the prescient control of the chance score, a carefully outlined hazard bend was developed, empowering the clear partition of patients into prognostic subgroups and giving a visual representation of their unique survival directions, eventually highlighting the potential clinical utility of this chance stratification approach in directing personalized treatment techniques and progressing persistent results. The fastidious examination of quality expression information permitted for the stratification of qualities into tall- and low-risk categories, shedding light on the complex exchange between atomic marks and persistent prognosis, eventually giving important bits of knowledge into the fundamental instruments driving infection movement and treatment reaction. A comprehensive and thorough autonomous prognostic examination was conducted, utilizing both univariate and multivariate approaches to recognize variables with critical prognostic value. To survey the unfair control of diverse factors in determining understanding prognosis, a recipient working characteristic (ROC) bend was carefully built and analyzed, empowering a comprehensive assessment of their prescient execution and potential clinical utility. A point by point chart was fastidiously arranged to viably visualize the comes about, and each patient's characteristic score was accurately calculated in understanding with the set up scoring scale. The total score encouraged the expectation of persistent survival rates at differing time focuses. By fastidiously developing a calibration bend and thoroughly evaluating its nearness to the perfect bend, we were able to inexact the exactness of our demonstrate in foreseeing persistent prognosis with a tall degree of exactness. For the reason of approval, the LIRI-JP record, containing information from 27 November 2019, was fastidiously downloaded from the ICGC database. This comprehensive information source empowered us to thoroughly confirm the survival contrasts between bunches with up- and downregulated HSP90AB1 quality expression and to comprehensively approve the precision and vigor of the developed prognostic model [2].

3. Results

As shown in **Figure 1**, an in-intensity exam of medical records from the TCGA database confirmed a notably better expression of the HSP90AB1 gene within the HCC institution than the normal institution ($P < 0.001$).

Figure 2 meticulously illustrates the composition of the tumour microenvironment in HCC patients by visualizing the distribution of diverse immune cell types within each individual. Each cell type is meticulously assigned a unique colour, facilitating identification and quantification.

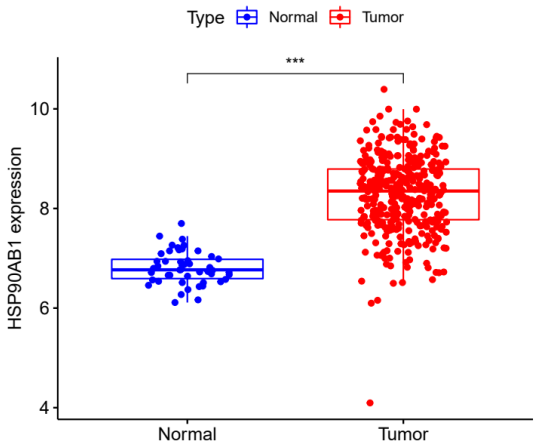

Figure 1. An in-intensity exam of medical records from the TCGA database confirmed a notably better expression of the HSP90AB1 gene within the HCC institution than the normal institution ($P < 0.001$). Box plot of HSP90AB1 expression levels in tumor tissue compared to normal tissue.

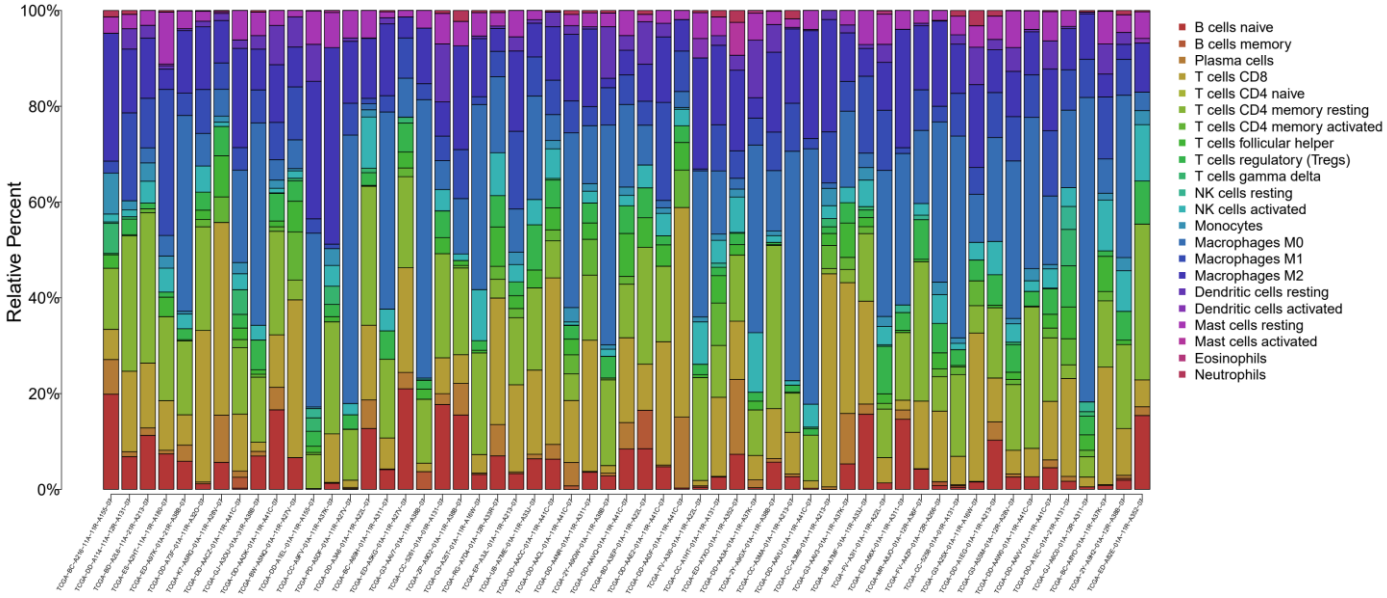

Figure 2. Different immune cell types in each HCC patient.

A meticulous analysis of data obtained from the TCGA database revealed a complex network of correlations among diverse immune cell types within the HCC microenvironment. The results displayed in **Figure 3** uncovered a striking inverse relationship between macrophage M0 cells and CD8+ T cells, supported by robust statistical evidence. This observation suggests that macrophage M0 cells may play a role in creating an immunosuppressive tumour microenvironment, which could impede the proper activation and function of cytotoxic CD8+ T cells. On the other hand, a statistically significant positive correlation was found between CD4+ memory-activated T cells and CD8+ T cells, indicating a possible synergistic interaction between these two cell types in mounting an effective anti-tumor immune response. These results offer insights into the intricate relationships among various immune cell types within the HCC microenvironment.

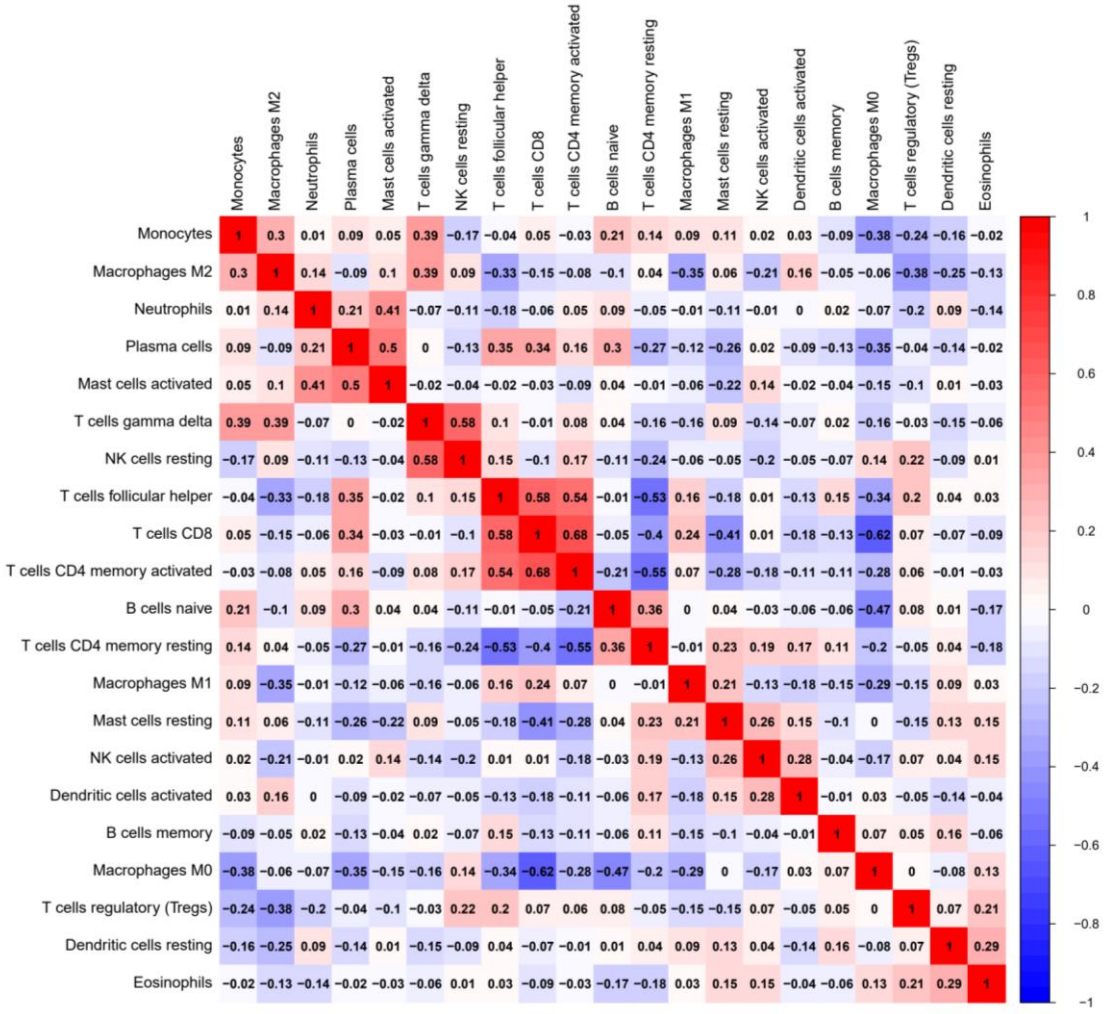

Figure 3. Heatmap of correlation among different immune cells in the HCC patients.

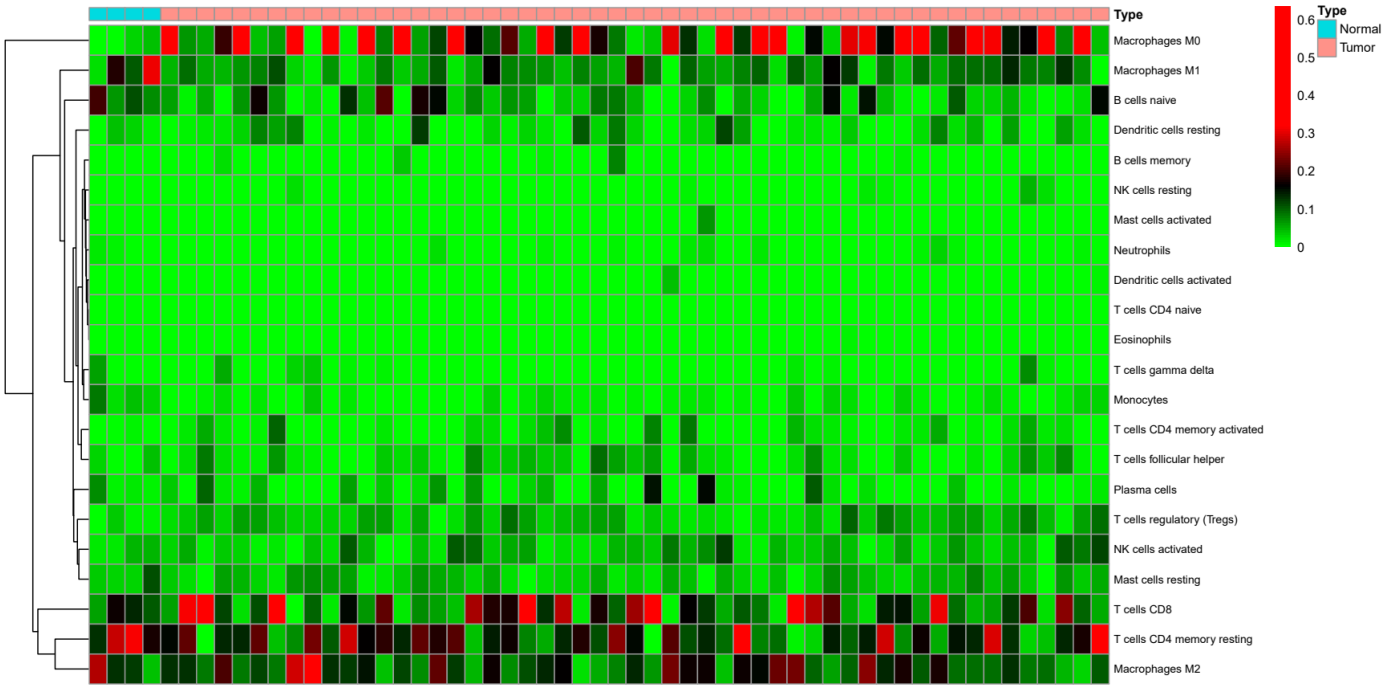

Figure 4. Different immune cells between normal and HCC patients.

A comprehensive analysis of the heat map in **Figure 4** reveals a distinct differentiation in immune cell profiles between normal and HCC groups. The Macrophage M0 content is particularly interesting, as it exhibits a statistically significant reduction in the normal group compared to the HCC group.

A thorough comparative analysis was conducted to assess the disparities in immune cell infiltration patterns between healthy liver tissues and hepatocellular carcinoma (HCC) samples, aiming to elucidate the potential role of the tumour microenvironment in HCC pathogenesis and progression. **Figure 5** was generated to visually compare the abundance of various immune cell types in both groups. This plot represents the distribution and density of immune cell populations, allowing for a detailed examination of the immune landscape in normal and HCC tissues. *P*-values were meticulously calculated and displayed above each group to ensure statistical rigour. Employing a stringent threshold of $P < 0.05$, a comprehensive screening of significantly different immune cell populations was performed. This analysis revealed a distinct differentiation between the two groups and the abundance of Naïve B cells, Naïve CD4 T cells, regulatory T cells (Tregs), monocytes, and macrophages M0. The HCC group was particularly interesting, as it demonstrated a statistically significant elevation in the abundance of Tregs and macrophages M0 compared to the normal group.

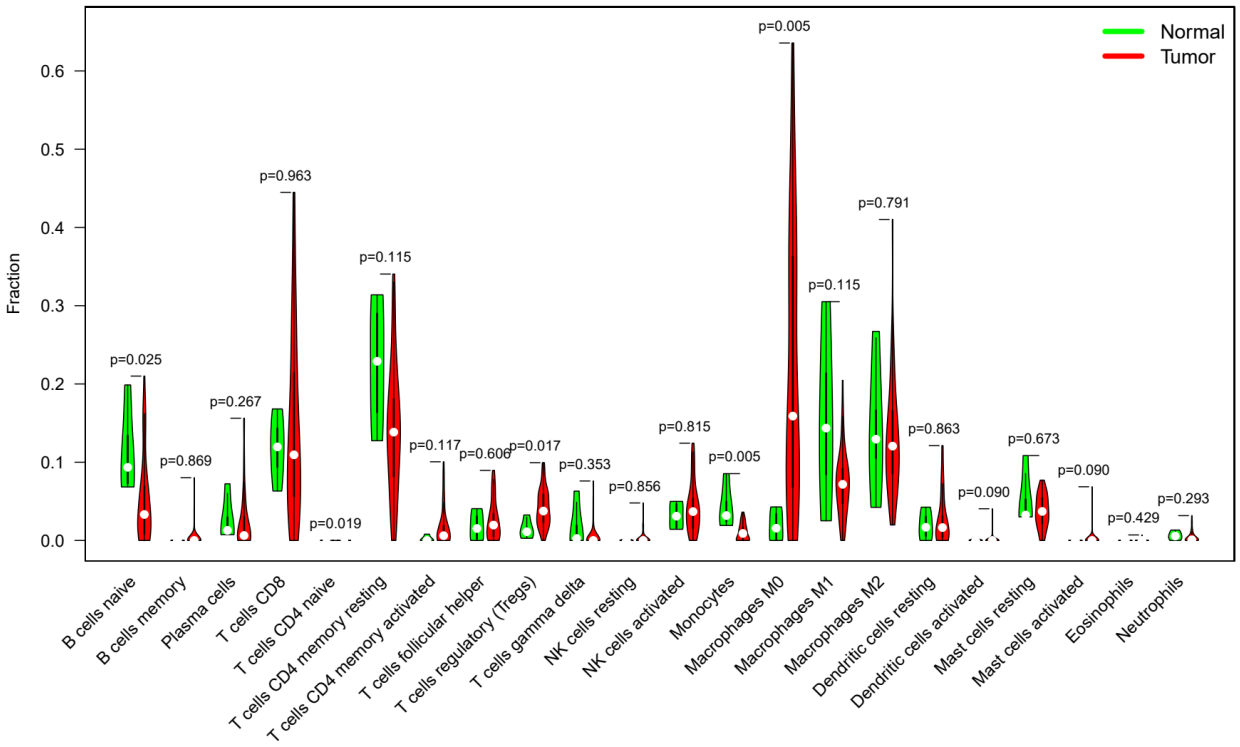

Figure 5. A comprehensive analysis of immune cell infiltration reveals significant variations between normal and tumour groups.

A meticulous analysis of **Figure 6** reveals a statistically significant reduction in the infiltration of neutrophils and CD8+ T cells within the HCC microenvironment when the HSP90AB1 copy number reaches the Arm-level Gain ($P < 0.05$). **Figure 6** shows how the infiltration of neutrophils and CD8+ T lymphocytes inside the HCC

microenvironment is affected by different HSP90AB1 copy levels. Our results show a substantial reduction in CD8+ T cell infiltration is associated with increased copies of HSP90AB1. Cytotoxic T cells are vital for identifying and eliminating cancer cells; hence, their decline is paramount. On the other hand, there was no discernible pattern to neutrophil infiltration, which may point to a more nuanced interaction dependent on other elements inside the TME.

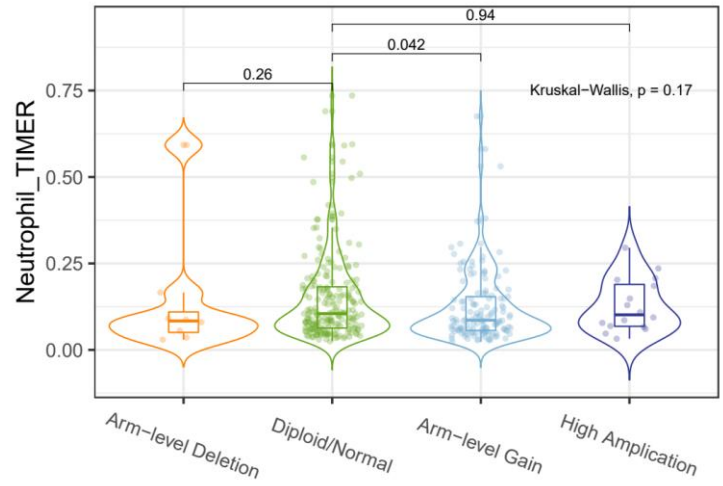

(a)

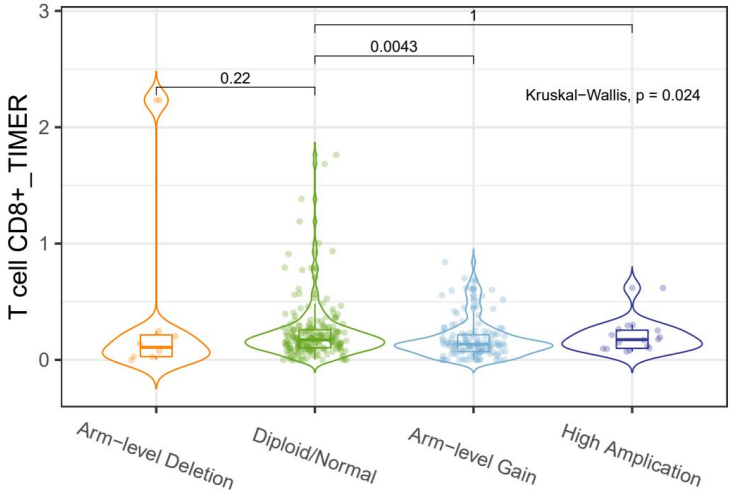

(b)

Figure 6. (a) An investigation into the impact of differing HSP90AB1 copy numbers on the infiltration of neutrophils cells within the HCC microenvironment; **(b)** an investigation into the impact of differing HSP90AB1 copy numbers on the infiltration of CD8+ T cells within the HCC.

The oxidative-phosphorylation pathway was active when HSP90AB1 gene expression was downregulated ($p < 0.05$) according to the GSEA enrichment analysis (**Figure 7**).

A thorough exam of **Figure 8** exhibits a statistically enormous superb correlation between HSP90AB1 gene expression and the presence of TGD and TCM_CD4 cells inside the HCC microenvironment. Conversely, HSP90AB1 expression confirmed a

sturdy terrible correlation, with statistical significance, with numerous immune molecular populations, inclusive of NK cells, Tem_CD8, Th1 cells, Th17 cells, MDSC, pDC, Treg, Act_B, Tem_CD4, macrophages, Mem_B, neutrophils, eosinophils, Imm_B, NKT cells, and Th2 cells. This inverse courting shows that HSP90AB1 might exert a suppressive impact at the infiltration and pastime of those immune molecular subsets, probably contributing to an immunosuppressive tumour microenvironment in HCC. The statistical association between the number of lymphocytes and HSP90AB1 expression levels is shown in **Figure 8**. A lower number of lymphocytes in the tumour microenvironment (TME) is linked to increased HSP90AB1 expression. This decrease may cause the immune system to become less effective, allowing the tumour to grow more aggressively by avoiding detection. Reducing the number of lymphocytes, especially T cells, highlights the immunosuppressive function of HSP90AB1. These cells are essential for launching an efficient anti-tumour response.

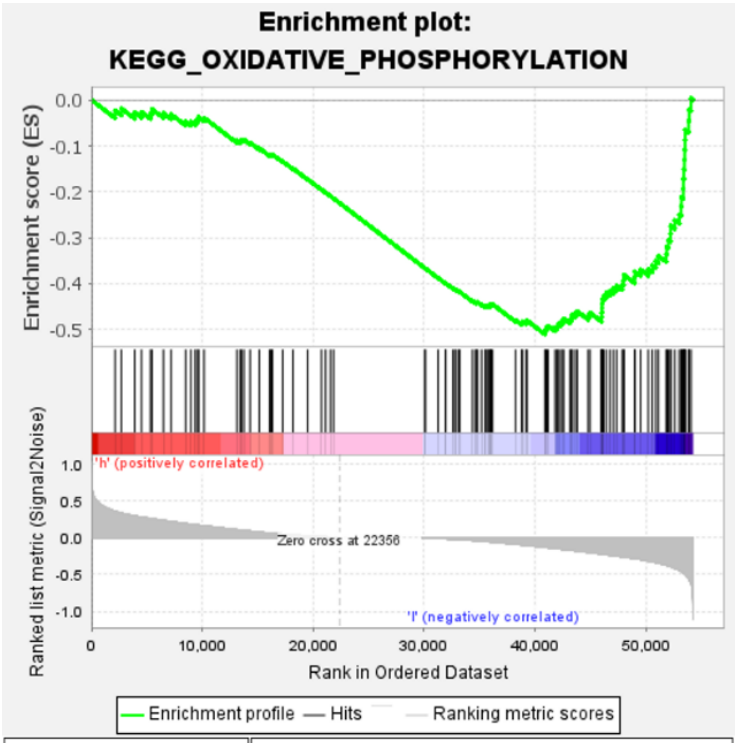

Dataset	HSP90AB1.HSP90AB1.cls#h_versus_l.HSP90AB1.cls#h_versus_l_repos
Phenotype	HSP90AB1.cls#h_versus_l_repos
Upregulated in class	l
GeneSet	KEGG_OXIDATIVE_PHOSPHORYLATION
Enrichment Score (ES)	-0.5101812
Normalized Enrichment Score (NES)	-1.4851172
Nominal p-value	0.037623763

Figure 7. GSEA enrichment analysis of HSP90AB1.

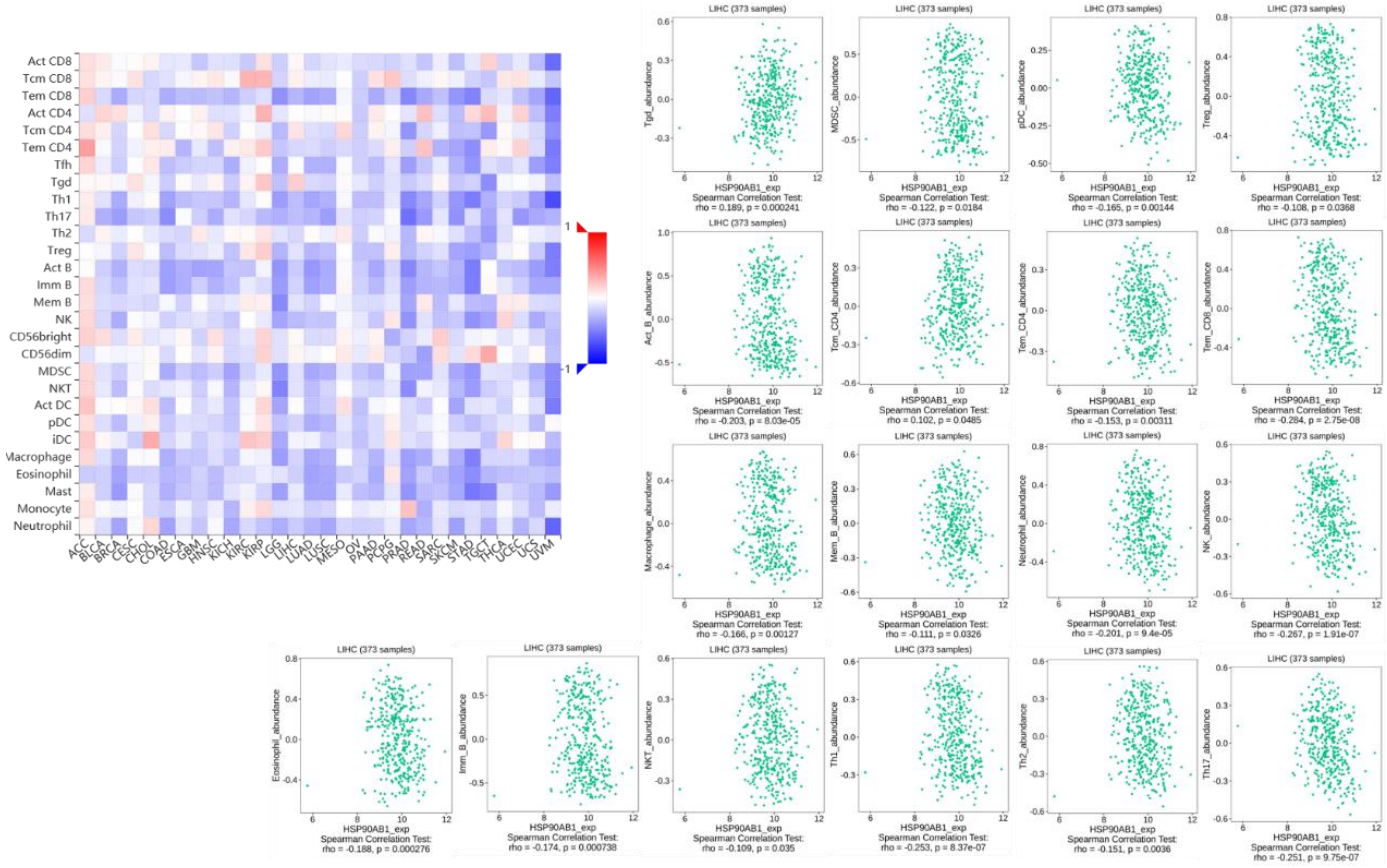

Figure 8. There is a significant statistical correlation between the expression of the HSP90AB1 gene and the number of lymphocytes.

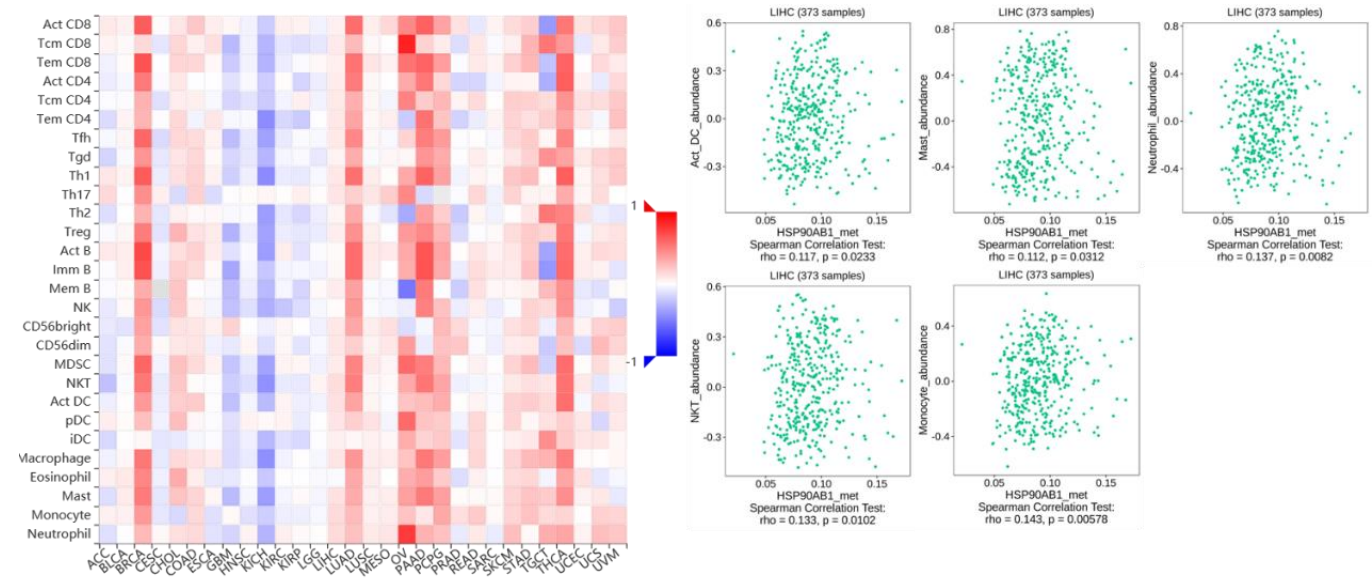

Figure 9. Correlation among the methylation of the HSP90AB1 gene and lymphocyte count.

As shown in **Figure 9**, a statistically enormous correlation exists among HSP90AB1 gene methylation and lymphocyte count, with a superb correlation found for ACT_DC, mast cells, neutrophils, NKT cells, and monocytes in the HCC microenvironment.

A complete evaluation of **Figure 10** exhibits a statistically enormous terrible

correlation between HSP90AB1 gene replica quantity and lymphocyte count, suggesting a capacity function of HSP90AB1 replica quantity in suppressing precise immune molecular populations in the HCC microenvironment. Notably, ACT_B, ACT_DC, IDC, macrophages, Tregs, mast cells, MDSC, MEM_B, monocytes, Th17, neutrophils, NKT, pDC, TCM_CD4, Th1, TCM_CD8, TEM_CD4, TEM_CD8, and TFH cells exhibited a terrible correlation with HSP90AB1 replica quantity. Further research into this correlation's underlying mechanisms and healing implications is warranted. The correlation between the number of copies of the HSP90AB1 gene and the number of lymphocytes is further investigated in **Figure 10**. According to the findings, a reduced number of lymphocytes in the tumor microenvironment (TME) is related to increased copies of the HSP90AB1 gene. This lends credence to the idea that HSP90AB1 influences the presence and function of immune cells in tumour environments.

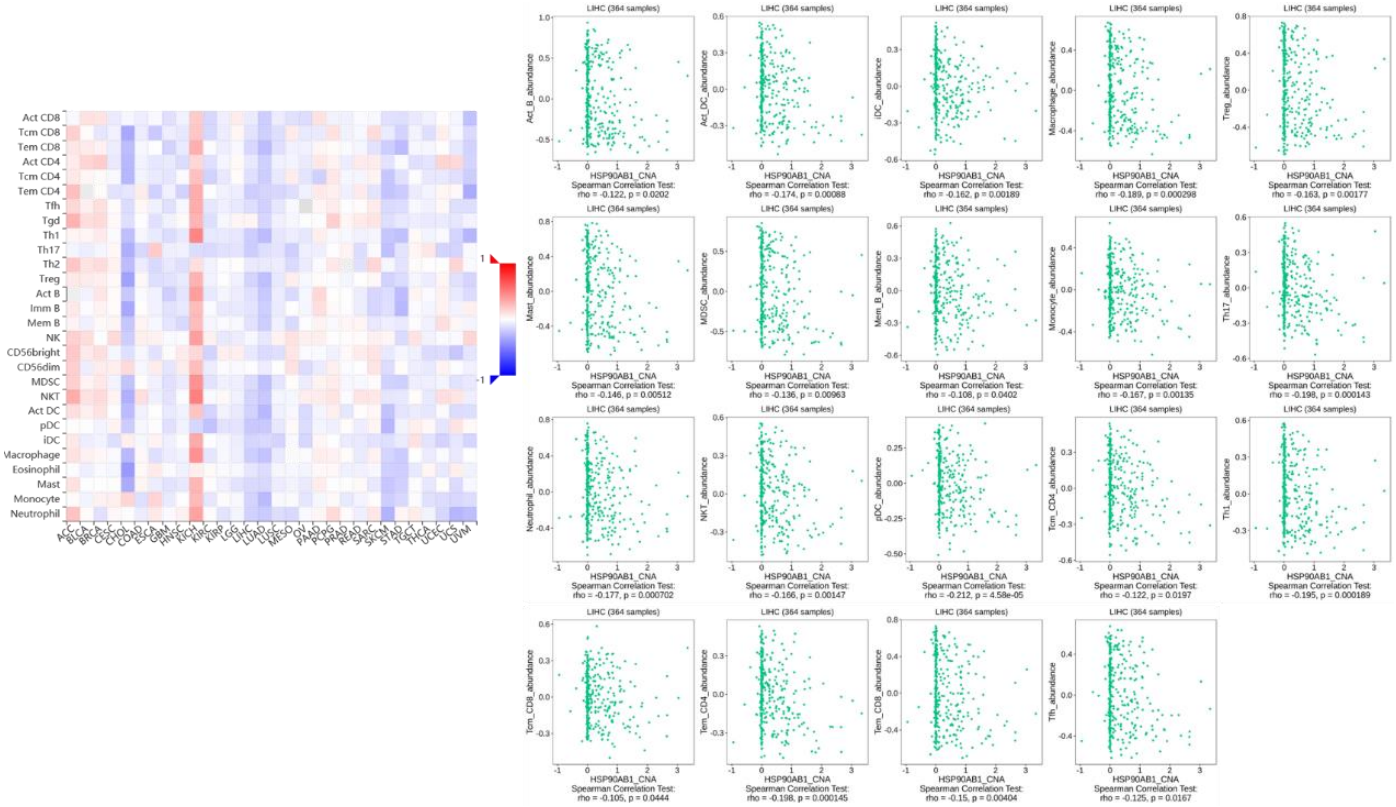

Figure 10. Correlation among the replica quantity of the HSP90AB1 gene and lymphocyte count.

The thorough research of gene expression styles recognized an enormous inverse affiliation among HSP90AB1 and key immune-stimulatory genes, including CD28, CD40, CXCL12, IL6, KLRK1, TMEM173, TNFRSF8, TNFRSF14, TNFSF13, TNFSF13B, TNFSF14, and HSP90AB1. These statistically supported consequences propose that HSP90AB1 might also have an important function in dampening immune-activating signaling pathways in the HCC tumor microenvironment, all likely due to the suppression of anti-tumour immune responses. Conversely, a superb correlation was found for CD276, MICB, TNFRSF4, and TNFSF9 genes, probably indicating a complicated interaction between HSP90AB1 and immune regulation. Further research into those correlations' underlying mechanisms and healing

implications is warranted. A correlational assessment between immune-stimulating genes and HSP90AB1 expression is shown in **Figure 11**. According to our findings, the expression of genes involved in immunological activation and stimulation, such as IFNG (interferon gamma) and TNF (tumor necrosis factor), is adversely linked with increased HSP90AB1 levels. The activation of immune responses against tumour cells critically depends on these genes. When their expression is low with high levels of HSP90AB1, it suggests that the immune system is being repressed.

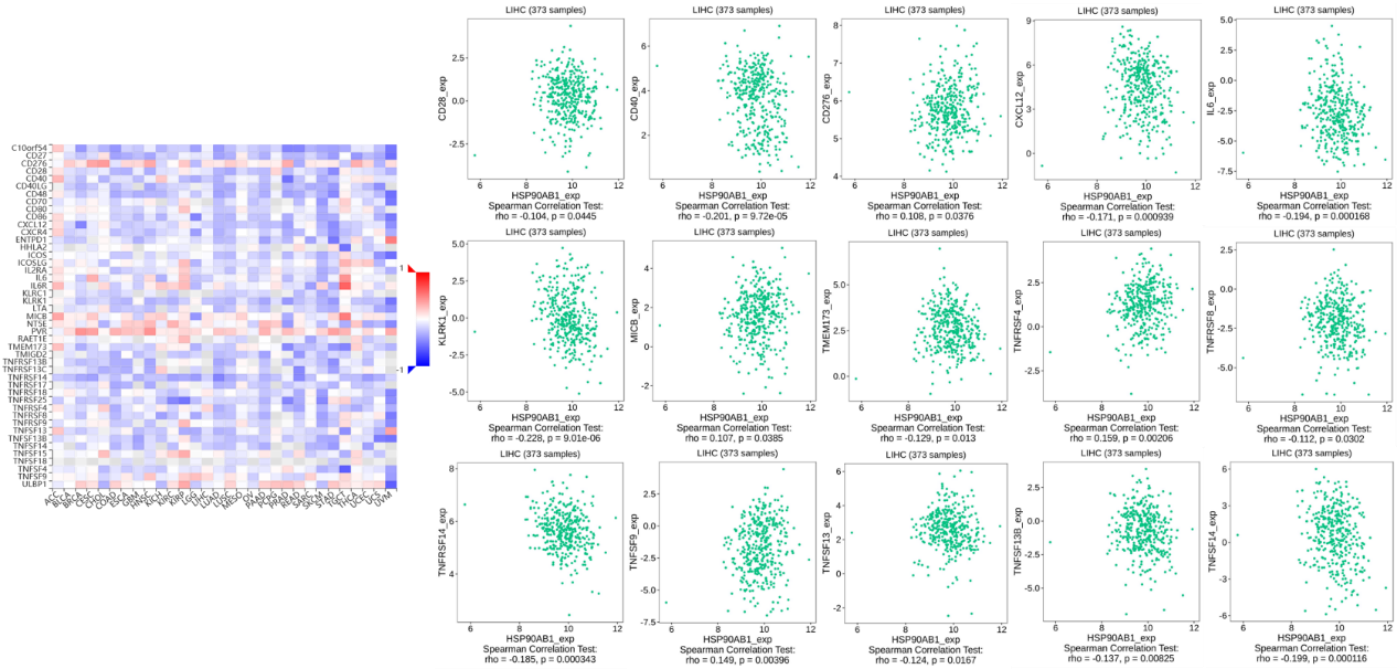

Figure 11. Correlational evaluation among the HSP90AB1 gene and immune-stimulating genes.

The in-intensity exam of gene expression records exposed a first-rate inverse courting among HSP90AB1 and numerous immune checkpoint genes, inclusive of BTLA, CD96, CD160, CD244, CD274, KDR, LAG3, PDCD1LG2, and TGFbr1. These findings, supported by sturdy statistical evaluation, suggest that HSP90AB1 might contribute to the established order of an immunosuppressive milieu in the HCC tumour microenvironment, probably facilitating tumour immune evasion and progression. This locating aligns with preceding research highlighting the involvement of HSP90AB1 in immune evasion mechanisms. Further research into this correlation's underlying mechanisms and healing implications is warranted. The relationship between immunosuppressive gene expression and HSP90AB1 is shown in **Figure 12**. When HSP90AB1 levels are high, genes that decrease immunological responses, such as transforming growth factor-beta 1 (TGFB1) and interleukin-10 (IL10), are expressed. HSP90AB1 may improve the immunosuppressive tumour microenvironment (TME), allowing tumour immune evasion and development due to the increased expression of these immunosuppressive genes and high levels of HSP90AB1.

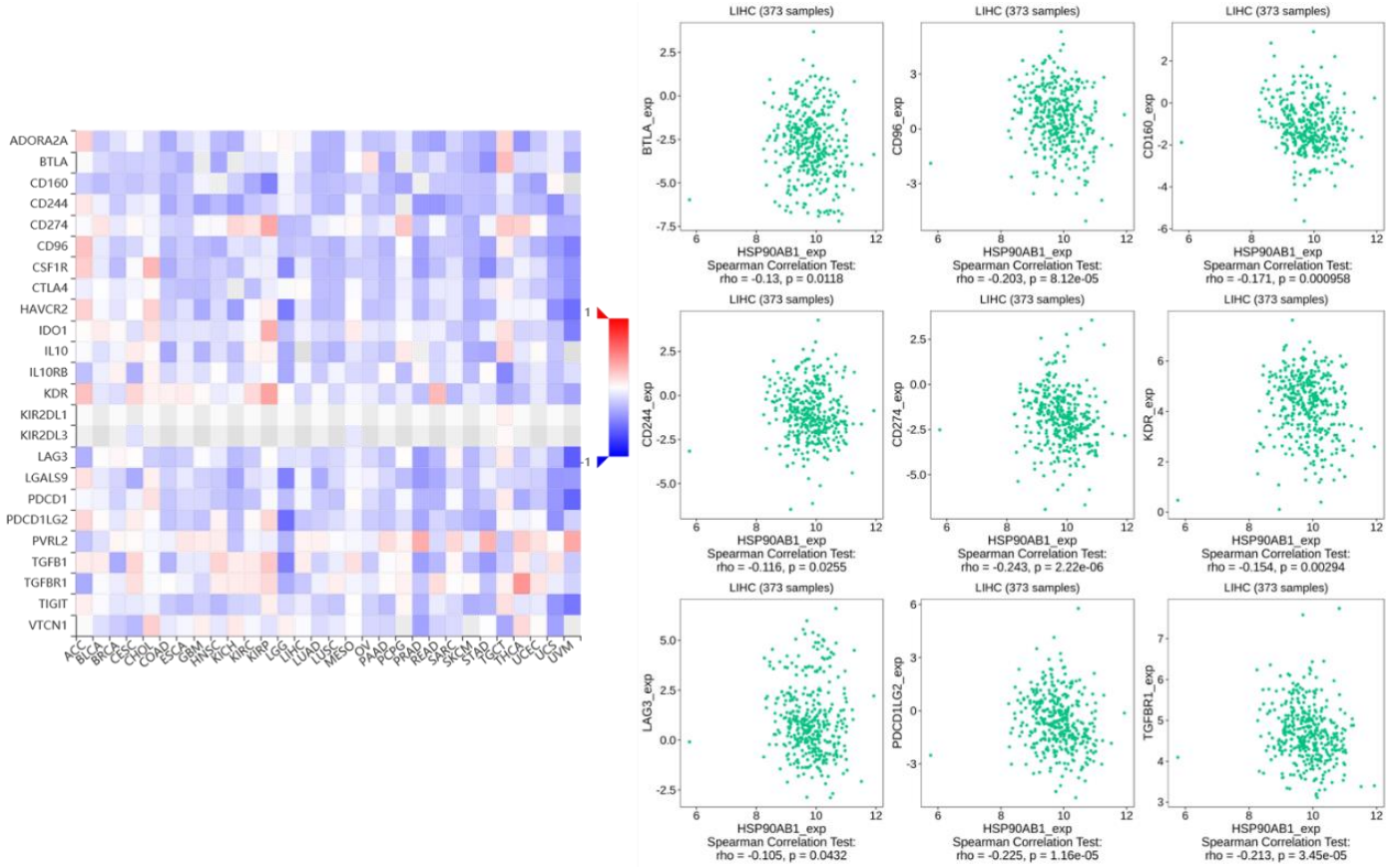

Figure 12. Correlational evaluation among the HSP90AB1 gene and immunosuppressive genes.

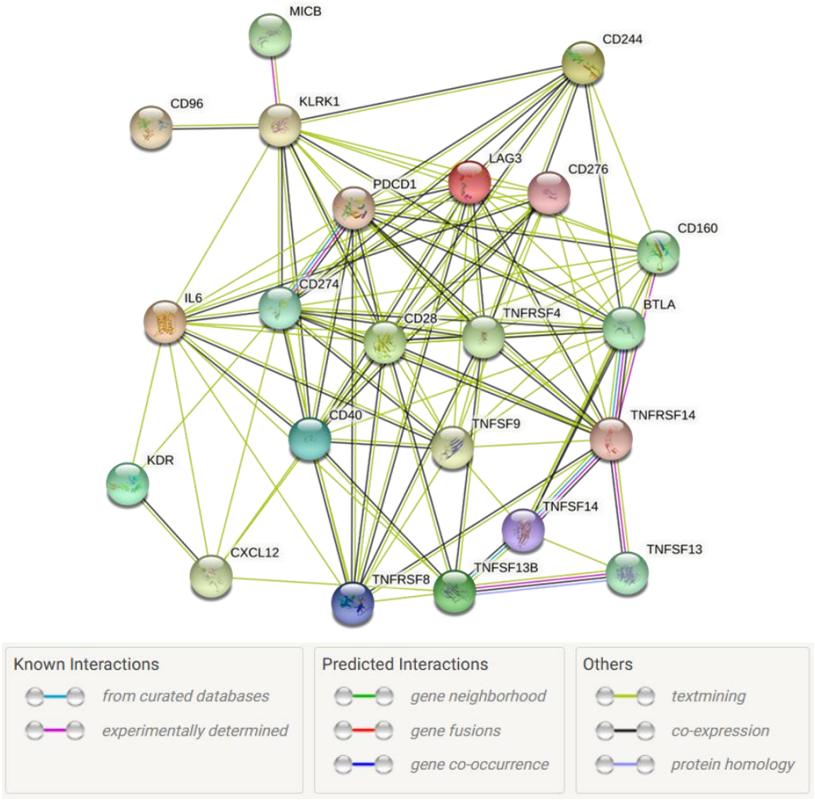

Figure 13. Protein-interplay community of immune-stimulating genes and immunosuppressive genes associated with the HSP90AB1 gene.

As shown in **Figure 13**, a certain protein interplay community was built to explain the tricky interaction among immune-stimulating and immunosuppressive genes related to HSP90AB1. The community discovered a complicated panorama of interactions through colourful traces connecting the genes. This visualization affords precious insights into the capacity mechanisms through which HSP90AB1 modulates immune responses in the HCC microenvironment. Further research into the useful implications of those interactions is warranted.

Using the web-primarily based totally gene set analysis toolkit, GO feature statistical evaluation was completed on genes inside the protein interplay community. The results were shown in **Figure 14**. Functional genes have been filtered with FDR values of <0.05, and the number of genes involved in each function is represented at the top.

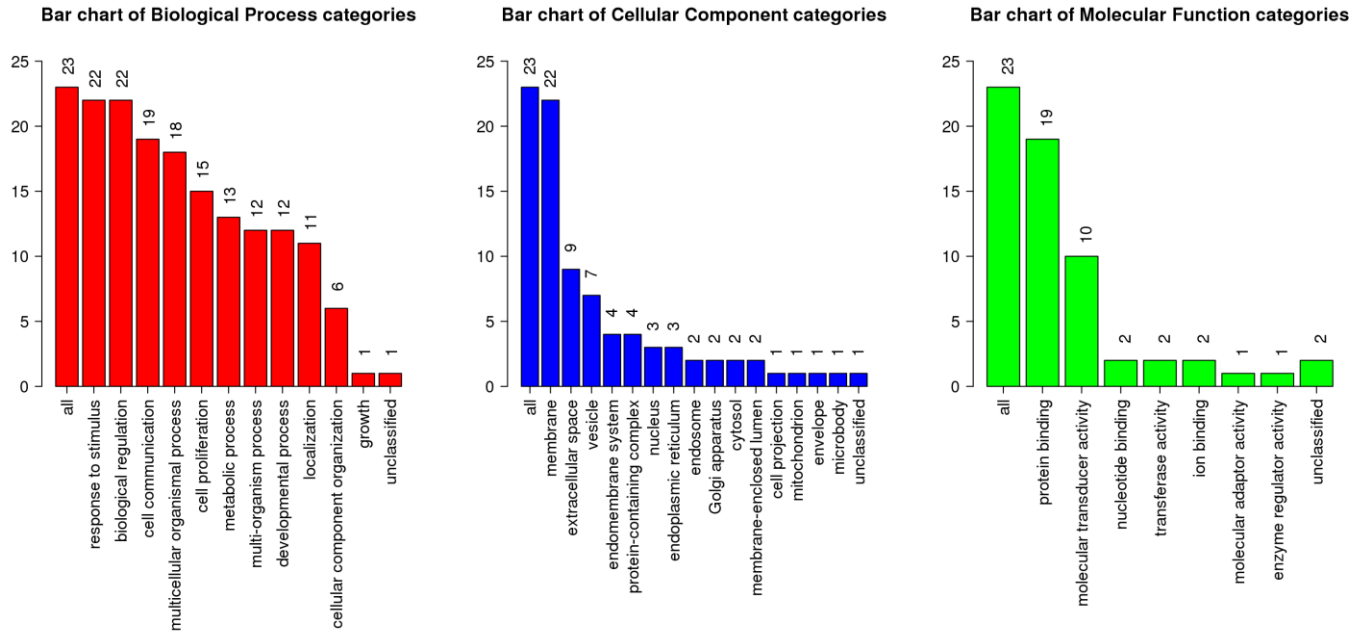

Figure 14. GO features statistical evaluation of genes inside the protein-interplay community.

As shown in **Figure 15**, a specific evaluation of the protein interplay community using the web-primarily based totally gene set analysis toolkit discovered many extensively enriched pathways, as displayed in the volcano map. The enriched pathways, together with cytokine-cytokine receptor interplay, an intestinal immune community for IgA production, rheumatoid arthritis, mobile adhesion molecules (CAMs), NF-kappa B signaling pathway, and malaria, recommend that HSP90AB1 participates in a complicated internet of mobile methods in the HCC tumour microenvironment. These findings underscore the capacity function of HSP90AB1 in modulating immune responses, inflammation, mobile-mobile interactions, and signaling cascades, which can also contribute to the improvement and development of HCC. Further research into the practical implications of those pathways is warranted to clarify their capacity roles in HCC improvement and development.

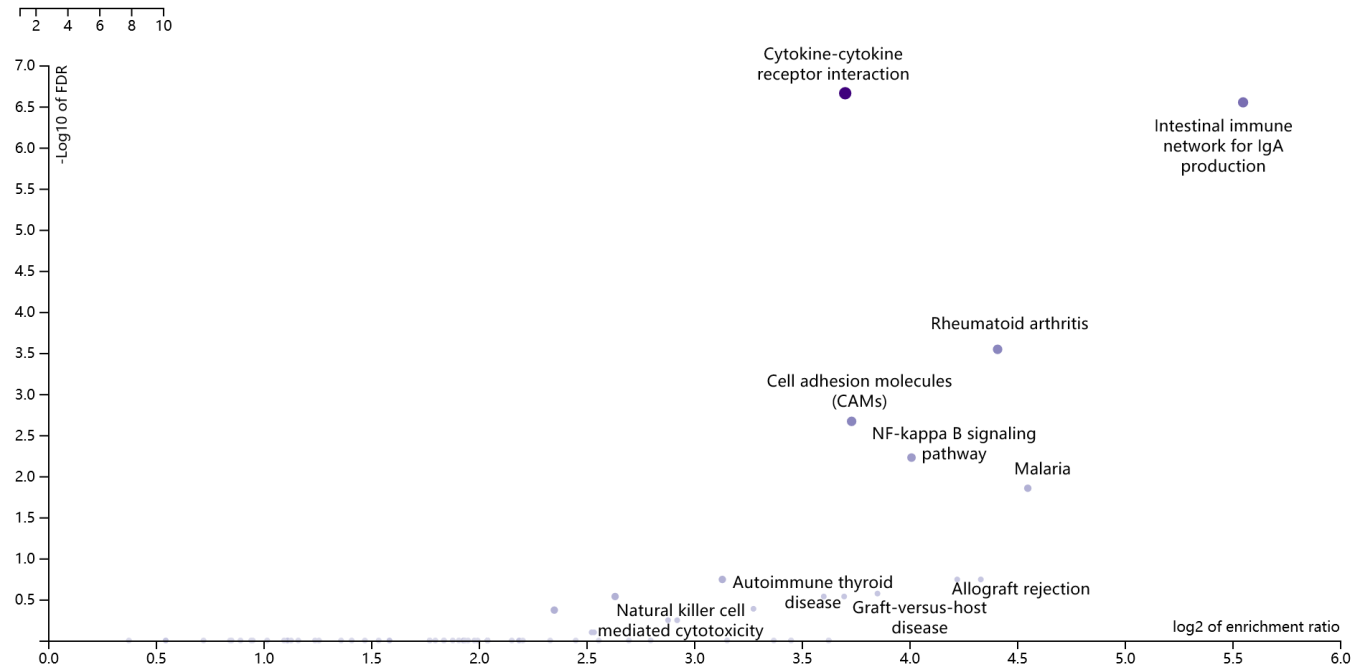

Figure 15. Pathways of extensively enriched genes are recognized primarily based on GO characteristic statistical analyses.

Table 1 gives the genes related to the analysis of HCC sufferers, which have been recognized from the protein interplay community (**Figure 13**) using an importance threshold of $P < 0.05$. The table proves that the KDR gene became a prognostically low-danger gene, while CD276, MICB, and TNFRSF4 genes have been prognostically excessive-danger genes. Genes associated with HCC patient prognosis found by protein-interaction network analysis are listed in **Table 1**. The kinase inserts domain receptor (KDR), MHC class I polypeptide-related sequence B (MICB), and CD276 (also known as B7-H3) were singled out because of the strong correlations between them and patient outcomes. These genes are relevant to HCC development and prognosis because they are important in angiogenesis, immune response regulation, and tumour immune evasion.

Table 1. The genes related to the prognosis of HCC patients in the protein-interaction network.

ID	HR	HR.95L	HR.95H	*p*-value
KDR	0.773	0.635	0.941	0.010
CD276	1.284	1.019	1.619	0.034
MICB	1.292	1.019	1.638	0.035
TNFRSF4	1.321	1.053	1.656	0.016

The analysis-associated genes recognized inside the preliminary screening have been evaluated extra to refine the prognostic version. The ensuing version integrates the coefficients of every decided-on gene, as specific in **Table 2**, permitting the computation of individualized danger ratings for every affected person. This method enhances the version's predictive accuracy and scientific applicability in assessing

affected person analysis. The prognostic model that was created utilizing KDR, MICB, and CD276 is shown in **Table 2**. The gene expression data and clinical outcomes in HCC patients were used to build this model. To classify patients into high-risk and low-risk categories, the model uses the expression levels of these genes to generate risk scores.

Table 2. The prognostic model of selected prognosis-related genes.

ID	Coef	HR	HR.95L	HR.95H	*p*-value
KDR	−0.226	0.798	0.655	0.972	0.025
MICB	0.217	1.243	0.981	1.575	0.072
TNFRSF4	0.223	1.249	0.993	1.572	0.057

As illustrated in **Figure 16**, the Kaplan-Meier survival evaluation efficiently stratifies sufferers into awesome danger classes primarily based on the prognostic version evolved in this study. The survival curves illustrate the version's potential to distinguish between low-danger and excessive-danger-affected person corporations. The log-rank check validates the statistical importance of this distinction ($P < 0.001$), emphasizing the version's reliability in predicting affected person outcomes. The extensively better survival possibility within the low-danger organization than the excessive-danger organization underscores the prognostic version's scientific price in figuring out sufferers with higher outcomes. This danger stratification method gives precious insights for personalized remedy planning, aid allocation, and affected person counselling. The prognostic version's performance, as validated via survival curves, emphasizes its capacity to help scientific decision-making and enhance standard affected person care by permitting focused interventions and surveillance techniques primarily based totally on character danger profiles.

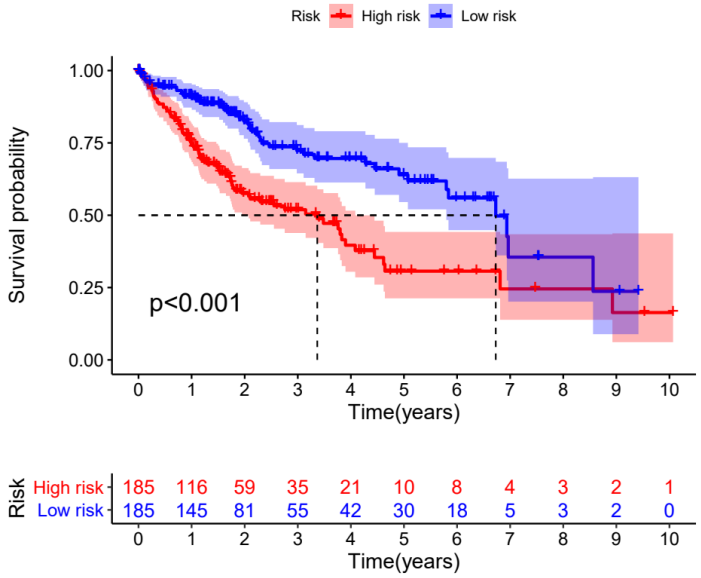

Figure 16. The Kaplan-Meier plot, primarily based on TCGA data, demonstrates that the prognostic version can efficiently classify HCC sufferers into excessive- and low-danger corporations with awesome survival outcomes, underlining its capacity for scientific software in individualized danger evaluation and remedy planning.

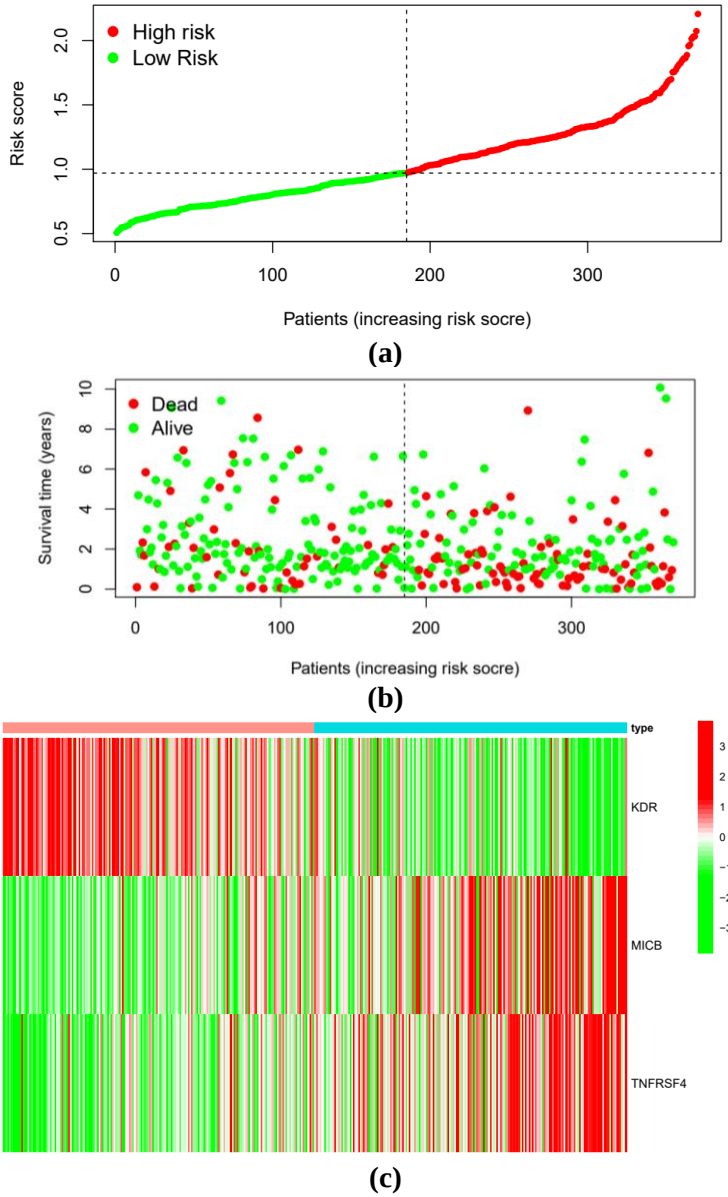

Figure 17. Using the prognostic version, the danger curve was generated for the excessive- and low-danger HCC-affected person corporations within the TCGA database. **(a)** A risk scoring curve that shows the distribution of patients' risk scores; **(b)** a scatter plot that illustrates the relationship between patients' survival time and risk scores; **(c)** a heatmap that shows the expression levels of different genes in various patients.

Figure 17a indicates a regular upward push in affected person danger ratings from left to right, dividing sufferers into excessive- and low-danger corporations primarily based on median ratings. **Figure 17b** illustrates a slow boom in affected person danger ratings from left to right, with better ratings connected to better mortality rates. In **Figure 17c**, the evaluation indicates low expression of the KDR gene and excessive expression of MICB and TNFRSF4 genes inside the excessive-danger organization, indicating the jobs of KDR as a low-danger gene and MICB, TNFRSF4 as excessive-danger genes in HCC improvement in the TCGA database.

The risk curve for high-risk and low-risk HCC patient groups within the TCGA database was constructed using the prognostic model, as shown in **Figure 17**. The risk curve shows distinct variations in survival outcomes, which divides the two groups. Higher levels of KDR, MICB, and CD276 expression are associated with worse survival rates in this group of patients. Elevated levels of these genes' expression point to a more aggressive tumour phenotype characterized by heightened angiogenesis, immunological evasion, and suppression. Patients with lower expression levels of these genes are considered to be in the low-risk category and have a greater chance of surviving. A more powerful anti-tumour immune response and less aggressive tumour activity will likely help these individuals.

An unbiased prognostic evaluation of the installed version was carried out, with **Figure 18a** displaying the wooded area plot from the single-element evaluation and **Figure 18b** from the multi-element evaluation. Both analyses yielded *P* values much less than 0.01, demonstrating that the prognostic version is powerful and may be independently applied for prognostic exams without affecting different traits.

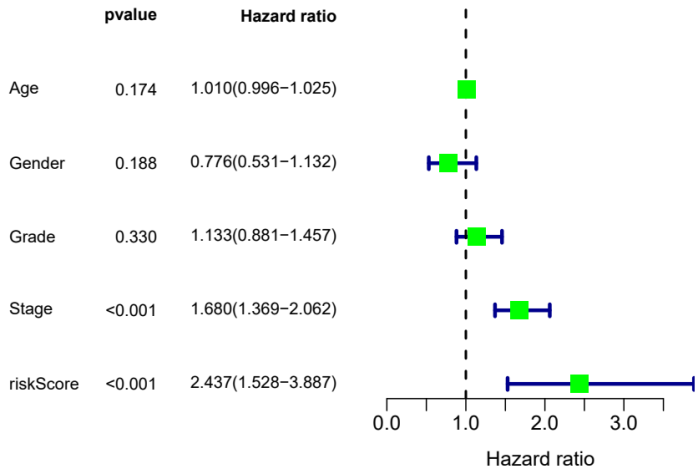

(a)

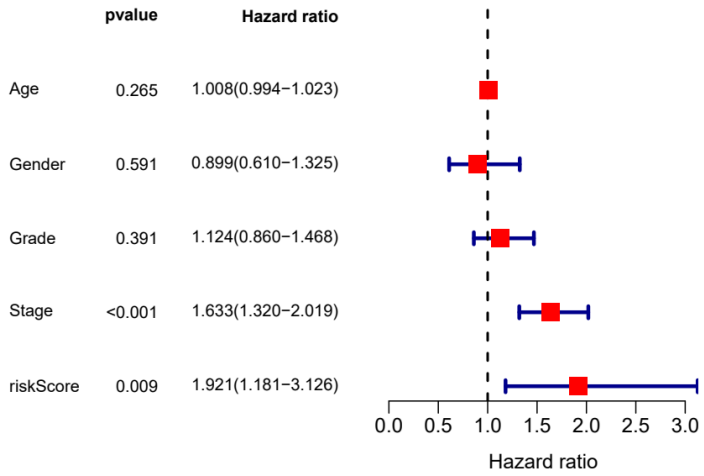

(b)

Figure 18. (a) Independent single-element prognostic analyses have been carried out using the installed version within the TCGA database; **(b)** independent multi-element prognostic analyses have been carried out using the installed version within the TCGA database.

The ROC curve in **Figure 19** exhibits that the vicinity below the risk + clinical curve is the most substantial, exceeding the regions below the stage and risk curves. This locating shows that the prognostic version, whilst included with extra scientific traits, gives particular and dependable predictions for affected person survival outcomes. Compared to other clinical features in the TCGA database, **Figure 19** shows the prognostic model's receiver operating characteristic (ROC) curve. The ROC curve is one way to visually see the model's diagnostic power. Accuracy in classifying patients as high- or low-risk is shown by the area under the receiver operating characteristic (ROC) curve (AUC). One indicator of good prognostic performance is an increased AUC. Cancer grade and stage are clinical characteristics that may be used to compare the ROC curve of the prognostic model and ensure the model's accuracy. To improve prognosis accuracy beyond standard pathological criteria, it is recommended to include molecular data (KDR, MICB, CD276) into the prognostic model if the AUC is greater.

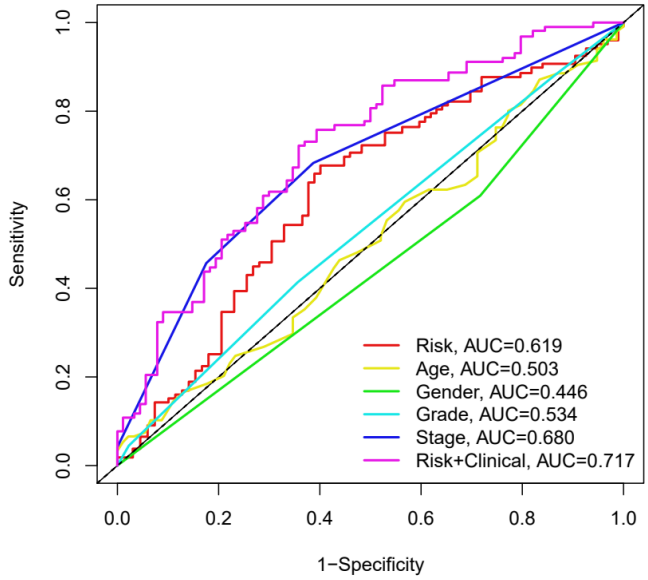

Figure 19. This figure offers the receiver operating characteristic (ROC) curve of the prognostic version and different scientific traits inside the TCGA database.

Figure 20a functions as an in-depth nomogram applied for the survival evaluation of HCC sufferers. It assigns rankings to every scientific trait primarily based on a single-aspect scoring scale; those rankings are then summed to derive a complete affected person rating. This comprehensive rating helps predict survival rates at one, two, and three years. In **Figure 20b**, the calibration curve carefully parallels the prediction curve, substantiating the accuracy of the built prognostic version.

The prognostic version was carried out to categorize sufferers inside the ICGC database into low- and excessive-threat corporations. The survival curves in **Figure 21** display a higher analysis for low-threat sufferers than excessive-threat sufferers ($P < 0.05$).

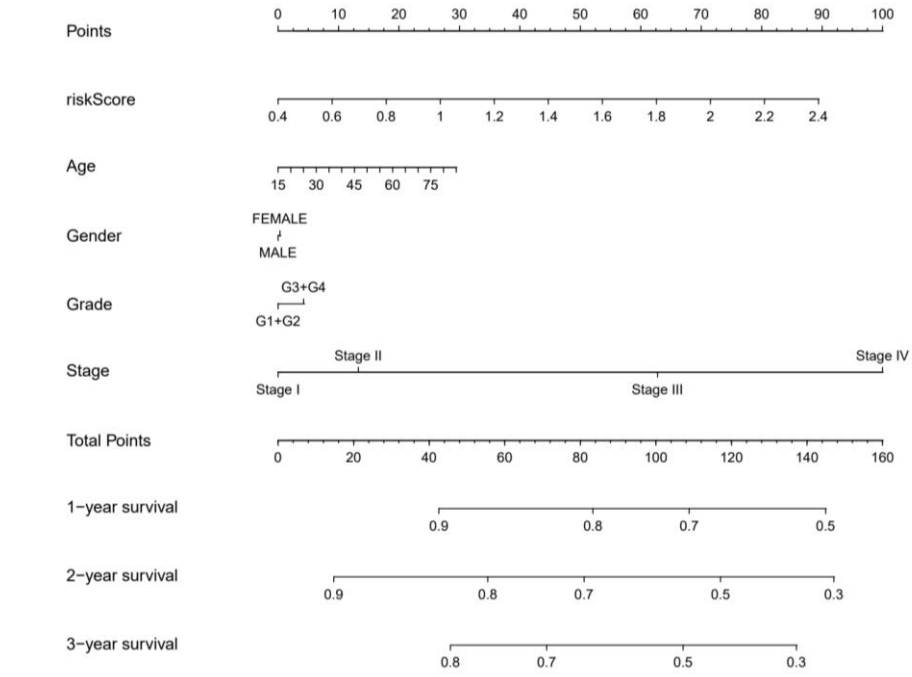

(a)

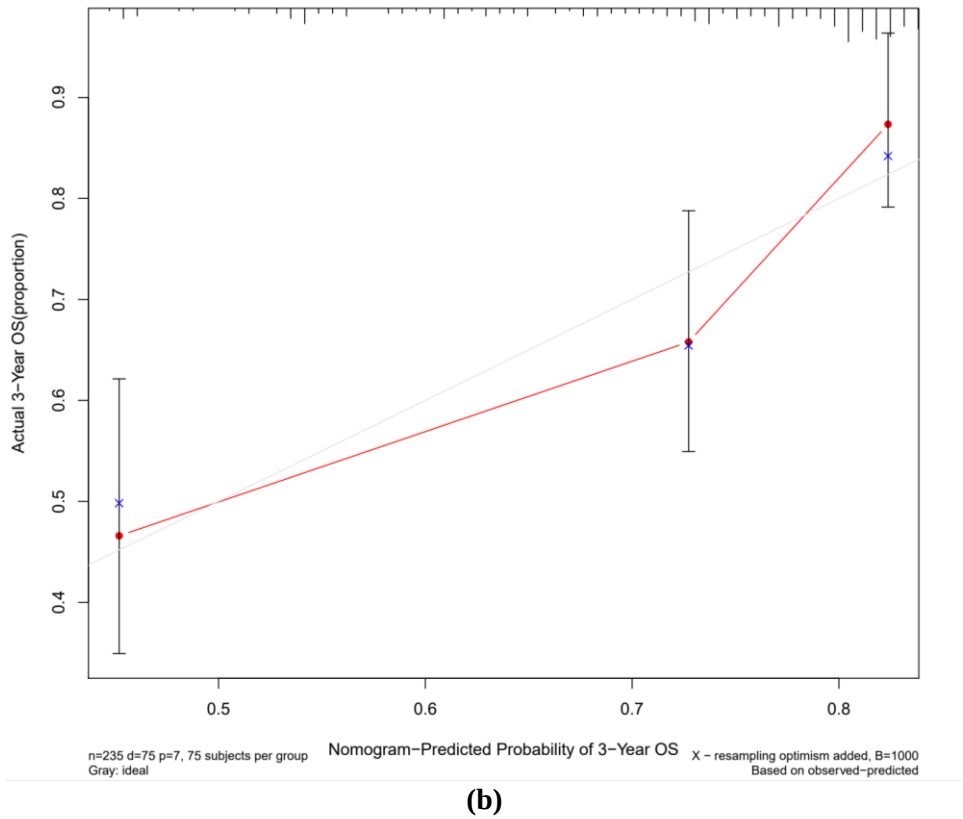

(b)

Figure 20. (a) The nomogram of the prognostic version inside the TCGA database; **(b)** the calibration curves of the prognostic version inside the TCGA database.

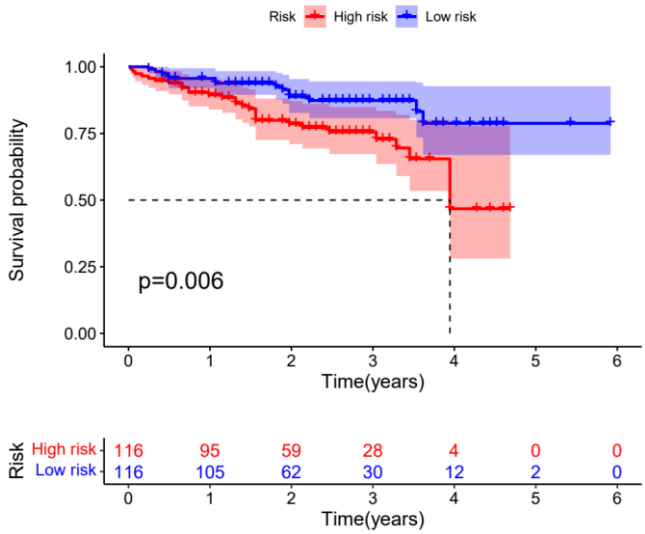

Figure 21. The survival curve for excessive- and low-threat HCC-affected person corporations is categorized through the prognostic version inside the ICGC database.

The ICGC database functions as a threat curve in **Figure 22a**, wherein the abscissa represents sufferers organized sequentially, and the ordinate, their corresponding threat rankings, which grow from left to right. **Figure 22b** suggests a correlation between the development alongside the curve and increasingly more affected person deaths, with the vertical axis measuring survival time. The threat heatmap in **Figure 22c** illustrates the expression styles of KDR, MICB, and TNFRSF4 genes in excessive- and low-threat corporations, highlighting the decreased expression of the KDR gene inside the excessive-threat group.

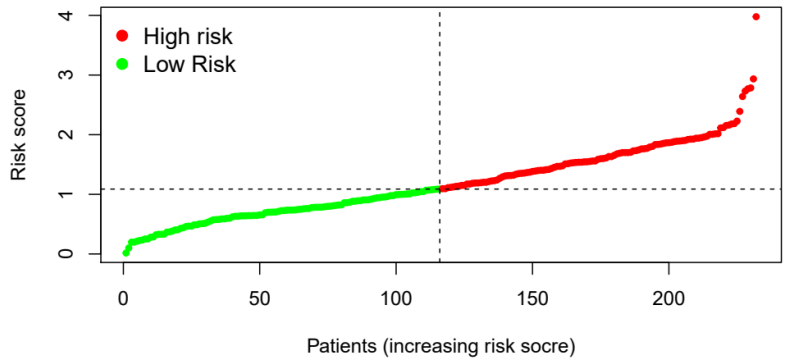

(a)

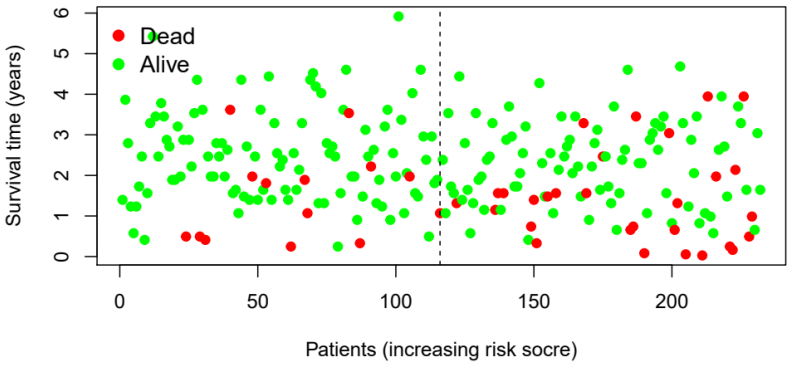

(b)

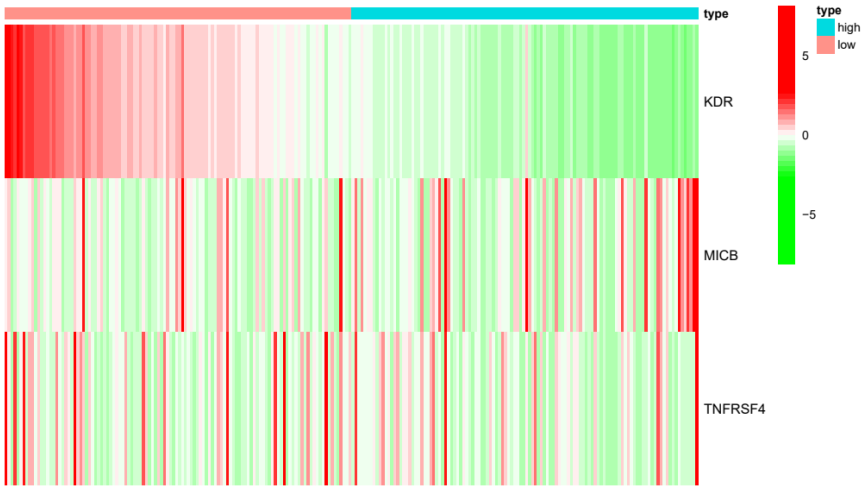

(c)

Figure 22. The threat curve for excessive- and low-threat HCC-affected person corporations classified through the prognostic version inside the ICGC database. **(a)** A risk scoring curve that shows the distribution of patients' risk scores; **(b)** a scatter plot that illustrates the relationship between patients' survival time and risk scores; **(c)** a heatmap that shows the expression levels of different genes in various patients.

An intensive impartial prognostic evaluation was performed to verify whether the prognostic version derived from the ICGC database information should be characteristic independently of different scientific traits. **Figure 23a** offers a woodland plot from the univariate evaluation, demonstrating that each Stage and risk score, with *P* values beneath 0.001, are giant impartial prognostic elements. Similarly, **Figure 23b** suggests the woodland plot from the multivariate evaluation, wherein those elements hold their importance with *P* values beneath 0.01. Consequently, each Stage and risk score are shown as legitimate for impartial prognostic use, becoming independent from different scientific traits. Using the existing model inside the ICGC database, **Figure 23** displays the results of single-aspect and multi-aspect independent prognostic assessments. It assesses each factor's predictive importance separately, for example, KDR, MICB, CD276 expression, tumour grade, and stage. Considers several variables to ascertain their predictive power as a whole. Through this all-encompassing method, connections between molecular and pathophysiological factors may be discovered.

The ROC curve in **Figure 24** for the ICGC database suggests the vicinity below the curve, which shows the version's predictive accuracy for affected person survival. Specifically, the abscissa information is the fake nice price (1-specificity), even as the ordinate captures the real nice price (sensitivity). In comparison, the version's vicinity below the curve became considerably smaller than that of staging; however, it exceeded the regions related to different traits. Notably, the most important vicinity became determined whilst the version became hired together with different scientific traits, indicating advanced accuracy in survival prediction. **Figure 24** shows the receiver operating characteristic (ROC) curve that compares the prognostic model to clinical features in the ICGC database. We may look at the area under the curve (AUC) values in the ICGC database to verify the model's predictive accuracy. The model's trustworthiness is enhanced when the AUC values are consistent across various

datasets, such as TCGA and ICGC.

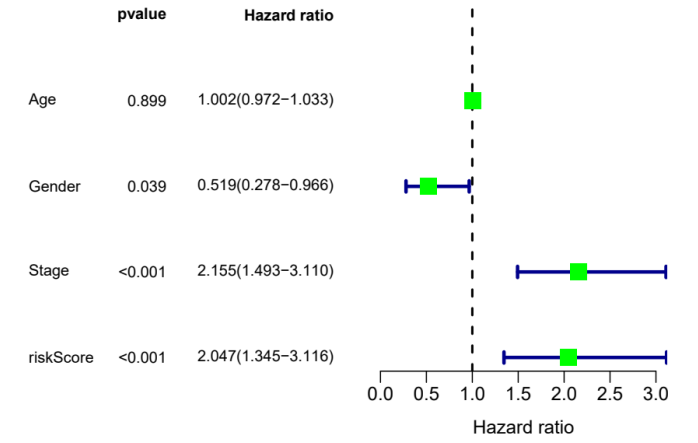

(a)

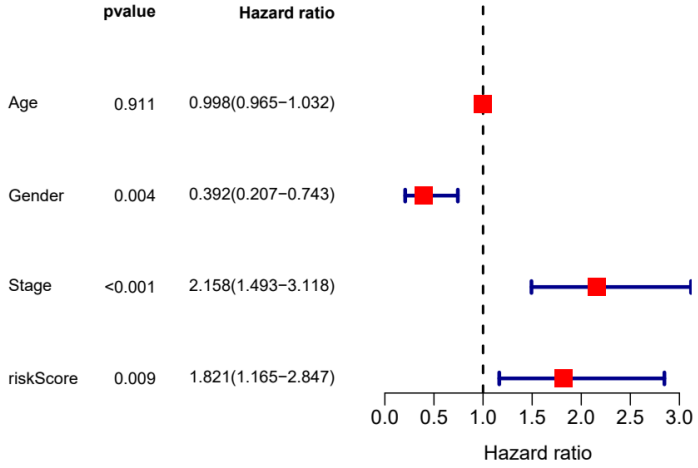

(b)

Figure 23. (a) The mounted prognostic version within the ICGC database became subjected to single-aspect impartial prognostic analysis; **(b)** the mounted prognostic version within the ICGC database became subjected to multi-aspect impartial prognostic analysis.

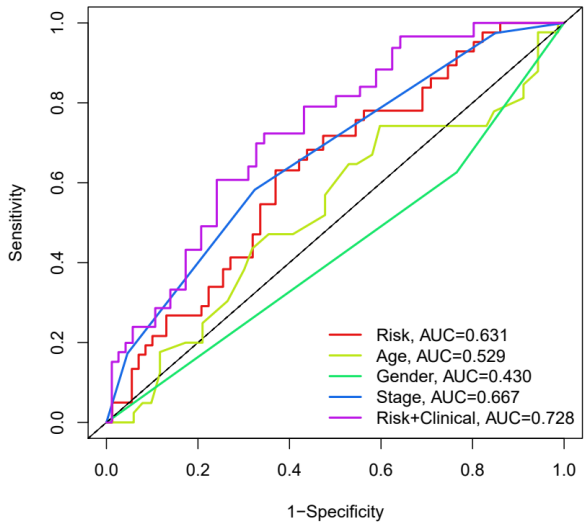

Figure 24. The ROC curve evaluating the prognostic version with scientific traits inside the ICGC database.

In the ICGC database, a single-aspect scoring scale was applied to assess every scientific trait of the sufferers, with the consequent rankings mixed to create a complete rating for predicting affected person survival rates, illustrated in **Figure 25a**. In **Figure 25b**, the calibration curve functions the version-anticipated mortality at the abscissa and the real mortality price at the ordinate. The near convergence of those curves demonstrates the excessive accuracy of the version's predictions.

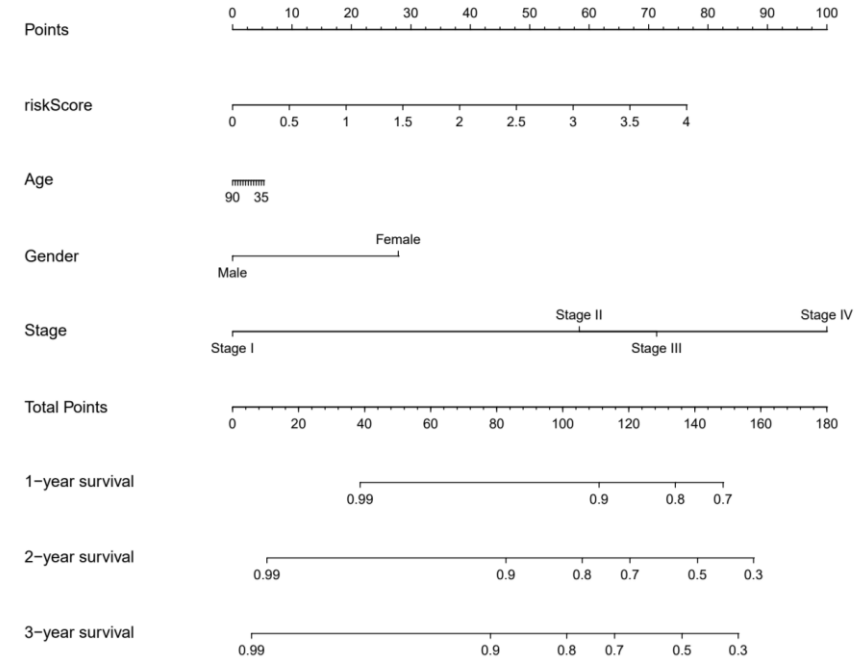

(a)

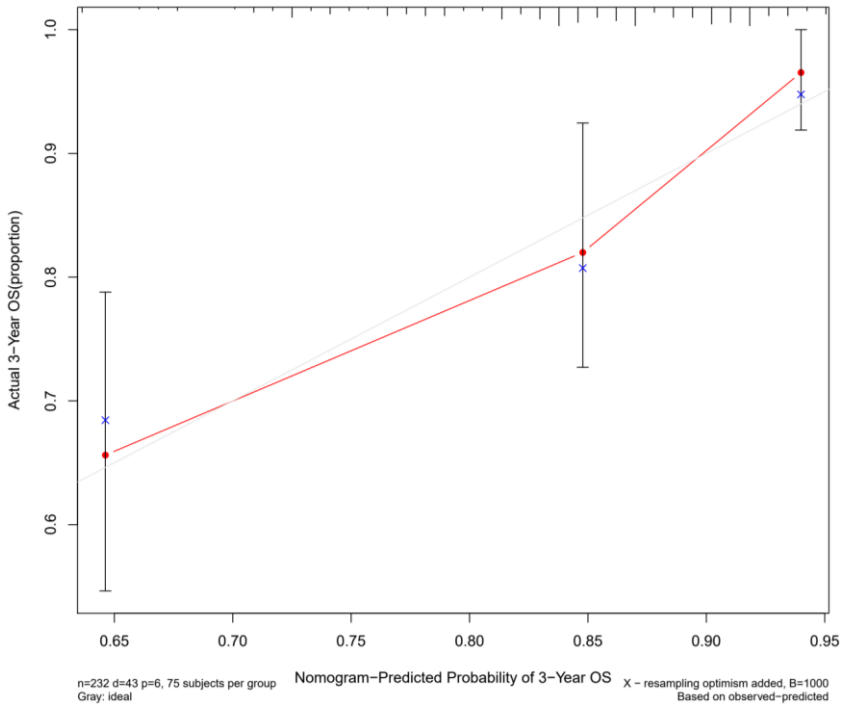

(b)

Figure 25. (a) The nomogram of the prognostic version inside the ICGC database; **(b)** the related calibration curves of the prognostic version inside the ICGC database.

4. Discussion

Later examinations have illustrated that HSP90 inhibitors essentially boost the adequacy of tumour immunotherapy, advertising promising roads for improved treatment results [14,15,30]. Be that as it may, the broad inhibitory impact of HSP90 inhibitors on different cellular targets has restricted their appropriation in far-reaching restorative hones. A few things have been investigated regarding the plausibility of decreasing the side impacts of Hsp90 inhibitors, one of which focuses on the HSP90AB1 subtype [10]. Subsequently, we comprehensively analyzed the impact of HSP90AB1 on the neighbourhood's safe reaction against HCC by utilizing information from the TCGA database. Numerous safe cells penetrated in HCC were found to be contrarily related to Hsp90β. The most unmistakable of these cells were a few CD8+ T cells, comparable to those of past thoughts about Hsp90 inhibitors [12]. Focusing on Hsp90AB1 for hindrance is anticipated to particularly increment the nearness of nearby executioner-safe cells inside hepatocellular carcinoma (HCC) tissues, opening up the restorative results of resistant checkpoint inhibitors. Assisting thinkers are required to investigate the significant impacts. We distinguished immunomodulatory qualities related to Hsp90AB1 and utilized a few immunostimulant and immunosuppressive qualities to create a prognostic demonstration. Investigation of understanding information from the TCGA database uncovered that Hsp90AB1 hindrance might significantly enhance understanding prognosis. Within the nearby microenvironment of hepatocellular carcinoma (HCC), NK cells, Tem_CD8 cells, Th1 cells, Th17 cells, MDSC cells, pDC cells, Treg cells, Act_B cells, Tem_CD4 cells, macrophages, Mem_B cells, neutrophils, eosinophils, Imm_B cells, NKT cells, and Th2 cells appeared a negative relationship with HSP90AB1 quality expression. Besides, an increment in HSP90AB1 duplicate number driven to diminished penetration of neutrophils and CD8+ T cells ($P < 0.05$), adjusting with discoveries from past thinks about HSP90 [14,15,30]. Suppressing HSP90AB1 increments CD8+ T cell penetration within the HCC microenvironment. GSEA enhancement examination uncovered that moo HSP90AB1 expression enacts the oxidative phosphorylation pathway, which is the essential vitality source for M2 macrophages [31]. Our inquiry has illustrated that oxygen-consuming glycolysis is a CD8+ T cell actuation biomarker. In contrast, youthful and memory (TMEM) cells predominantly rely on oxidative phosphorylation, highlighting the basic part of the mitochondrial digestion system in improving CD8+ TMEM cells. Moreover, most tumour-infiltrating T cells eventually show an exhaustion phenotype, characterized by a noteworthy misfortune of self-renewal capacity. In enacted T cells, smothering mitochondrial oxidative phosphorylation successfully stops cell multiplication and within the upregulation of qualities demonstrative of T cell disappointment. Alternately, avoiding mitochondrial oxidative stretch amid amplified T cell actuation keeps up T cell expansion and actuates qualities related to stem-like T begetter cells [32]. Additionally, restorative mediations that support REDOX balance have appeared to improve T cell self-renewal capabilities and open up anti-tumour safe capacities [33]. We utilized the screened MICB [34], KDR [5], and TNFRSF4 [35] genes to develop the prognostic model, in which KDR was a low-risk quality and MICB, TNFRSF4 qualities are high-risk qualities for HCC development according to the

TCGA database, but the degree of hereditary hazard is not clear within the ICGC database. KDR could be a low-risk prognostic quality in clinical information, and the results are exceedingly reliable within the clinical information from the two databases. Past reasons have recommended that the KDR quality advances angiogenesis in mouse liver cancer cells and relates to tumour movement, negating what comes about from the clinical information examination. This irregularity may arise from impediments within the current exploratory show, justifying encouraged examination. The prognostic demonstration, created by coordination immunoregulatory qualities connected to HSP90AB1 with extra clinical characteristics counting age, sex, review, and arrange, upgrades survival expectation precision and its unwavering quality has been affirmed through the ICGC database. Obtaining a more complex picture of how HCC develops and patient outcomes requires combining pathology findings with independent liver cancer prognostic data. Positioning molecular data inside the diseased landscape allows clinicians to enhance patient stratification, treatment plan personalization, prognosis accuracy, and therapeutic results. This complete approach highlights the importance of combining molecular insights with classical pathology to optimize the therapy of hepatocellular carcinoma.

5. Conclusion

In conclusion, targeting HSP90AB1 for inhibition significantly boosts the infiltration of CD8+ T cells in hepatocellular carcinoma (HCC) and mitigates the side effects typical of conventional Hsp90 inhibitors, suggesting their enhanced utility as therapeutic agents to augment the effectiveness of immunotherapy. Moreover, developing a prognostic model that integrates the expression of genes such as KDR, MICB, and TNFRSF4, in addition to other clinical traits, offers superior predictive accuracy for the prognosis of patients with HCC.

Ethical approval: Not applicable.

Conflict of interest: The authors declare no conflict of interest.

References

1. Bray F, Ferlay J, Soerjomataram I, et al. Global cancer statistics 2018: GLOBOCAN estimates of incidence and mortality worldwide for 36 cancers in 185 countries. CA Cancer J Clin. 2018; 68: 394-424.
2. Rheinbay E, Nielsen MM, Abascal F, et al. Analyses of non-coding somatic drivers in 2658 cancer whole genomes. Nature. 2020; 578: 102-111.
3. McGlynn KA, Petrick JL, El-Serag HB. Epidemiology of Hepatocellular Carcinoma. Hepatology. 2020; 73(S1): 4-13. doi: 10.1002/hep.31288
4. Greten TF, Mauda-Havakuk M, Heinrich B, et al. Combined locoregional-immunotherapy for liver cancer. Journal of Hepatology. 2019; 70(5): 999-1007. doi: 10.1016/j.jhep.2019.01.027
5. Llovet JM, Montal R, Sia D, et al. Molecular therapies and precision medicine for hepatocellular carcinoma. Nature Reviews Clinical Oncology. 2018; 15(10): 599-616. doi: 10.1038/s41571-018-0073-4
6. Proia DA, Kaufmann GF. Targeting Heat-Shock Protein 90 (HSP90) as a Complementary Strategy to Immune Checkpoint Blockade for Cancer Therapy. Cancer Immunology Research. 2015; 3(6): 583-589. doi: 10.1158/2326-6066.cir-15-0057
7. Miyata Y, Nakamoto H, Neckers L. The Therapeutic Target Hsp90 and Cancer Hallmarks. Current Pharmaceutical Design. 2013; 19(3): 347-365. doi: 10.2174/138161213804143725
8. Haase M, Fitze G. HSP90AB1: Helping the good and the bad. Gene. 2016; 575(2): 171-186. doi:

10.1016/j.gene.2015.08.063
9. Trepel J, Mollapour M, Giaccone G, et al. Targeting the dynamic HSP90 complex in cancer. Nature Reviews Cancer. 2010; 10(8): 537-549. doi: 10.1038/nrc2887
10. Khandelwal A, Kent CN, Balch M, et al. Structure-guided design of an Hsp90β N-terminal isoform-selective inhibitor. Nature Communications. 2018; 9(1). doi: 10.1038/s41467-017-02013-1
11. Tomašič T, Durcik M, Keegan BM, et al. Discovery of Novel Hsp90 C-Terminal Inhibitors Using 3D-Pharmacophores Derived from Molecular Dynamics Simulations. International Journal of Molecular Sciences. 2020; 21(18): 6898. doi: 10.3390/ijms21186898
12. Zavareh RB, Spangenberg SH, Woods A, et al. HSP90 Inhibition Enhances Cancer Immunotherapy by Modulating the Surface Expression of Multiple Immune Checkpoint Proteins. Cell Chemical Biology. 2021; 28(2): 158-168.e5. doi: 10.1016/j.chembiol.2020.10.005
13. Mbofung RM, McKenzie JA, Malu S, et al. HSP90 inhibition enhances cancer immunotherapy by upregulating interferon response genes. Nature Communications. 2017; 8(1). doi: 10.1038/s41467-017-00449-z
14. Kawabe M, Mandic M, Taylor JL, et al. Heat Shock Protein 90 Inhibitor 17-Dimethylaminoethylamino-17-Demethoxygeldanamycin Enhances EphA2 + Tumor Cell Recognition by Specific CD8+ T Cells. Cancer Research. 2009; 69(17): 6995-7003. doi: 10.1158/0008-5472.can-08-4511
15. Rao A, Taylor JL, Chi-Sabins N, et al. Combination Therapy with HSP90 Inhibitor 17-DMAG Reconditions the Tumor Microenvironment to Improve Recruitment of Therapeutic T cells. Cancer Research. 2012; 72(13): 3196-3206. doi: 10.1158/0008-5472.can-12-0538
16. Shimp SK, Chafin CB, Regna NL, et al. Heat shock protein 90 inhibition by 17-DMAG lessens disease in the MRL/lpr mouse model of systemic lupus erythematosus. Cellular & Molecular Immunology. 2012; 9(3): 255-266. doi: 10.1038/cmi.2012.5
17. Lin CC, Tu CF, Yen MC, et al. Inhibitor of Heat-shock Protein 90 Enhances the Antitumor Effect of DNA Vaccine Targeting Clients of Heat-shock Protein. Molecular Therapy. 2007; 15(2): 404-410. doi: 10.1038/sj.mt.6300014
18. Graner MW. HSP90 and Immune Modulation in Cancer. Hsp90 in Cancer: Beyond the Usual Suspects. 2016: 191-224. doi: 10.1016/bs.acr.2015.10.001
19. Yun TJ, Harning EK, Giza K, et al. EC144, a Synthetic Inhibitor of Heat Shock Protein 90, Blocks Innate and Adaptive Immune Responses in Models of Inflammation and Autoimmunity. The Journal of Immunology. 2011; 186(1): 563-575. doi: 10.4049/jimmunol.1000222
20. Song KH, Oh SJ, Kim S, et al. HSP90A inhibition promotes anti-tumor immunity by reversing multi-modal resistance and stem-like property of immune-refractory tumors. Nature Communications. 2020; 11(1). doi: 10.1038/s41467-019-14259-y
21. Haggerty TJ, Dunn IS, Rose LB, et al. A Screening Assay to Identify Agents That Enhance T-Cell Recognition of Human Melanomas. ASSAY and Drug Development Technologies. 2012; 10(2): 187-201. doi: 10.1089/adt.2011.0379
22. Zhang YJ, Yi DH. CDK1-SRC Interaction-Dependent Transcriptional Activation of HSP90AB1 Promotes Antitumor Immunity in Hepatocellular Carcinoma. Journal of Proteome Research. 2023; 22(12): 3714-3729. doi: 10.1021/acs.jproteome.3c00379
23. Xiao H, Wang B, Xiong H, et al. A novel prognostic index of hepatocellular carcinoma based on immunogenomic landscape analysis. Journal of Cellular Physiology. 2020; 236(4): 2572-2591. doi: 10.1002/jcp.30015
24. Hutter C, Zenklusen JC. The Cancer Genome Atlas: Creating Lasting Value beyond Its Data. Cell. 2018; 173(2): 283-285. doi: 10.1016/j.cell.2018.03.042
25. Li T, Fan J, Wang B, et al. TIMER: A Web Server for Comprehensive Analysis of Tumor-Infiltrating Immune Cells. Cancer Research. 2017; 77(21): e108-e110. doi: 10.1158/0008-5472.can-17-0307
26. Subramanian A, Tamayo P, Mootha VK, et al. Gene set enrichment analysis: A knowledge-based approach for interpreting genome-wide expression profiles. Proceedings of the National Academy of Sciences. 2005; 102(43): 15545-15550. doi: 10.1073/pnas.0506580102
27. Ru B, Wong CN, Tong Y, et al. TISIDB: an integrated repository portal for tumor-immune system interactions. Wren J, ed. Bioinformatics. 2019; 35(20): 4200-4202. doi: 10.1093/bioinformatics/btz210
28. von Mering C, Huynen M, Jaeggi D, et al. STRING: a database of predicted functional associations between proteins. Nucleic Acids Research. 2003; 31(1): 258-261. doi: 10.1093/nar/gkg034
29. Wang J, Duncan D, Shi Z, et al. WEB-based GEne SeT AnaLysis Toolkit (WebGestalt): update 2013. Nucleic Acids

Research. 2013; 41(W1): W77-W83. doi: 10.1093/nar/gkt439
30. Zhang Y, Ware MB, Zaidi MY, et al. Heat Shock Protein-90 Inhibition Alters Activation of Pancreatic Stellate Cells and Enhances the Efficacy of PD-1 Blockade in Pancreatic Cancer. Molecular Cancer Therapeutics. 2021; 20(1): 150-160. doi: 10.1158/1535-7163.mct-19-0911.
31. Griffiths HR, Gao D, Pararasa C. Redox regulation in metabolic programming and inflammation. Redox Biology. 2017; 12: 50-57. doi: 10.1016/j.redox.2017.01.023
32. Raud B, McGuire PJ, Jones RG, et al. Fatty acid metabolism in CD8+ T cell memory: Challenging current concepts. Immunological Reviews. 2018; 283(1): 213-231. doi: 10.1111/imr.12655
33. Vardhana SA, Hwee MA, Berisa M, et al. Impaired mitochondrial oxidative phosphorylation limits the self-renewal of T cells exposed to persistent antigen. Nature Immunology. 2020; 21(9): 1022-1033. doi: 10.1038/s41590-020-0725-2
34. Ferrari de Andrade L, Tay RE, Pan D, et al. Antibody-mediated inhibition of MICA and MICB shedding promotes NK cell-driven tumor immunity. Science. 2018; 359(6383): 1537-1542. doi: 10.1126/science.aao0505
35. Buchan SL, Rogel A, Al-Shamkhani A. The immunobiology of CD27 and OX40 and their potential as targets for cancer immunotherapy. Blood. 2018; 131(1): 39-48. doi: 10.1182/blood-2017-07-741025